

University of Louisville

## ThinkIR: The University of Louisville's Institutional Repository

---

Electronic Theses and Dissertations

---

8-2015

### Geotechnical laboratory characterization of sand-zeolite mixtures.

Hong Shang,  
*University of Louisville*

Follow this and additional works at: <https://ir.library.louisville.edu/etd>



Part of the [Civil Engineering Commons](#)

---

#### Recommended Citation

Shang,, Hong, "Geotechnical laboratory characterization of sand-zeolite mixtures." (2015). *Electronic Theses and Dissertations*. Paper 2210.

<https://doi.org/10.18297/etd/2210>

This Master's Thesis is brought to you for free and open access by ThinkIR: The University of Louisville's Institutional Repository. It has been accepted for inclusion in Electronic Theses and Dissertations by an authorized administrator of ThinkIR: The University of Louisville's Institutional Repository. This title appears here courtesy of the author, who has retained all other copyrights. For more information, please contact [thinkir@louisville.edu](mailto:thinkir@louisville.edu).

GEOTECHNICAL LABORATORY CHARACTERIZATION  
OF SAND-ZEOLITE MIXTURES

By

Hong Shang

A Thesis

Submitted to the Faculty of the  
J. B. Speed School of Engineering of the University of Louisville  
in Partial Fulfillment of the Requirements  
for the Degree of

Master of Science  
in Civil Engineering

Department of Civil and Environmental Engineering  
University of Louisville  
Louisville, Kentucky

August 2015

Copyright 2015 by Hong Shang

All rights reserved



GEOTECHNICAL LABORATORY CHARACTERIZATION  
OF SAND-ZEOLITE MIXTURES

By

Hong Shang

A Thesis Approved on

July 17, 2015

by the following Thesis Committee

---

Dr. Qian Zhao, Civil and Environmental Engineering

---

Dr. Thomas D. Rockaway, Civil and Environmental Engineering

---

Dr. Li Yang, Industrial Engineering

# DEDICATION

This thesis is dedicated to my parents

Mr. Lin Shang

And

Mrs. Lianhui Liu

Who have given me invaluable educational opportunities

## ACKNOWLEDGEMENT

I would like to thank my advisor, Dr. Qian Zhao, for his guidance and patience. I would also like to thank the other committee members, Dr. Thomas D. Rockaway and Dr. Li Yang for their comments and assistance. I would also like to express my thanks to my wife, Dan Qi, for her understanding and supporting. She encouraged me to overcome all the difficulties.

# ABSTRACT

TO QUANTIFY THE IMPACT OF ZEOLITE CONTENT AND  
COMPACTIVE EFFORT ON THE DENSITY, CONDUCTION AND  
COMPRESSIBILITY OF THE SAND-ZEOLITE MIXTURES.

Hong Shang

July 17, 2015

Zeolite and sand mixture is an ideal reactive filling material for the Permeable Reactive barrier (PRB) due to its higher hydraulic conductivity and sorption capacity. This study applied three ASTM standard tests to examine the geotechnical engineering properties of ASTM 20-30 sand and zeolite (clinoptilolite) mixtures with varying zeolite mass percentages (25%, 50% and 75%). Conducted lab tests including: Proctor compaction, hydraulic conductivity in rigid wall permeameter and one-dimensional consolidation. The goals of this study were to quantify the impact of zeolite content and compactive effort on the density, conduction and compressibility of the sand-zeolite mixtures.



# TABLE OF CONTENTS

DEDICATION .....	iii
ACKNOWLEDGEMENT .....	iv
ABSTRACT.....	v
LIST OF TABLES .....	viii
LIST OF FIGURES .....	ix
2. MATERIALS AND METHODS.....	6
2.1 <i>Materials</i> .....	6
2.1.1 Zeolite .....	6
2.1.2 ASTM 20-30 sand.....	8
2.2 <i>Test methods</i> .....	10
2. 2. 1 Lab tests arrangement .....	10
2. 2. 2 Particle size distribution and specific gravity test.....	11
2.2. 3 Compaction tests.....	12
2. 2. 4 Hydraulic conductivity tests.....	17
2.2. 5 Consolidation tests .....	23
3. RESULTS AND DISCUSSION .....	28
3.1 <i>Compaction</i> .....	28
3.1.1 Group 1 – 75% ASTM 20-30 sand and 25% zeolite.....	28
3.1.2 Group 2 – 50% ASTM 20-30 sand and 50% zeolite.....	30
3.1.3 Group 3 – 25% ASTM 20-30 sand and 75% zeolite.....	31
3.1.4 Comparison of three groups compaction test.....	32
3.2 <i>Hydraulic conductivity</i> .....	36
3.2.1 Hydraulic conductivity test for pre-compacted test samples with different water content of group1 – 75% ASTM 20-30 sand and 25% zeolite (clinoptilolite) .....	36

3.2.2	Hydraulic conductivity test for both pre-compacted (OPT) and uncompacted (same water content) samples with different zeolite (clinoptilolite) content.....	40
3.3	<i>Consolidation</i> .....	45
3.3.1	A representative results of the compression index and recompression index of Group 1 – 75% ASTM 20-30 sand and 25% zeolite mixtures.....	46
3.3.2	Compression and recompression indices of all three groups tested samples .....	49
3.3.3	The modulus of volume compressibility ( $m_v$ ).....	52
3.3.4	The coefficient of consolidation ( $C_v$ ).....	54
3.3.5	The relationships between the effective stress and strain of all three groups tested samples.....	58
4.	SUMMARY AND CONCLUSION .....	60
5.	SUGGESTION FOR FUTURE STUDY .....	62
	REFERENCES .....	63
	APPENDIX.....	68
	CURRICULUM VITA .....	75

## LIST OF TABLES

Table 2.1 Specific Gravity of sand-zeolite mixture .....	6
Table 2.2 Physical characteristics of sand and zeolite particles .....	10
Table 2.3 Testing matrix .....	11
Table 2.4 Sieves selected in the particle distribution test .....	12
Table 2.5 Loading and unloading procedures of the consolidation test .....	25
Table 3.1 Data acquisition of proctor compaction test results for three groups .....	34
Table 3.2 The data acquisition of hydraulic conductivity test results for different water content of 75% ASTM 20-30 sand and 25% zeolite mixtures compacted sample.....	37
Table 3.3 The data acquisition of hydraulic conductivity test results for both pre-compacted (OPT) and uncompacted (same water content of the OPT) test samples with different zeolite (clinoptilolite) content .....	41
Table 3.4 The void ratio and strain information at 10.14% water content(OPT) of 75% ASTM 20-30 sand and 25% zeolite mixtures compacted sample (Representative)....	46
Table 3.5 Compression and recompression indices of all the testing samples .....	49
Table 3.6 The modulus of volume compressibility (mv) of all the three groups.....	53
Table 3.7 The Coefficient of Consolidation (Cv) 10.14% water content(OPT) of 75% ASTM 20-30 sand and 25% zeolite mixtures compacted sample .....	54

## LIST OF FIGURES

Figure 2.3 The particle size distributions of the lab zeolite (Clinoptilolite).....	8
Figure 2.6 The particle size distributions of the lab ASTM20-30 sand.....	9
Figure 3.1 Compaction curve vs. different water content (75% sand vs. 25% zeolite).	28
Figure 3.2 Compaction curve vs. different water content (50% sand vs. 50% zeolite)	30
Figure 3.3 Compaction curve vs. different water content (25% sand vs. 75% zeolite).	31
Figure 3.5 Comparisons of three groups compaction curves.....	32
Figure 3.6 Log scale of hydraulic conductivity vs. different water content of 75% ASTM 20-30 sand and 25% zeolite mixtures compacted sample .....	37
Figure 3.7 Log scale of hydraulic conductivities vs. different water content of all the three groups compacted and uncompact samples and uncompact pure ASTM 20- 30 sand sample.....	41
Figure 3.8 Effective stress (kPa) log scal vs. oid ratio - e of 75% ASTM 20-30 sand and 25% zeolite mixtures at 10.14% water content of compacted sample .....	47
Figure 3.9 comparison of the void ratio vs. effective stress between the compacted and uncompact samples in group1 (25% clinoptilolite).....	50
Figure 3.10 Three group consolidation of the compacted samples on OPT .....	51
Figure 3.11 Three group consolidation of the uncompact samples with the same water content of each compacted OPT .....	51

Figure 3.12 Effective stress (kPa) log scal vs. void ratio  $e$  of group 1(25% clinoplilolite) with 10.14% water content (OPT) of compacted sample .....52

Figure 3.13 The representative of root time curves method of gropu 1 (75% ASTM 20-30 sand and 25% zeolite mixtures) at 10.14% water content of compacted sample .....55

Figure 3.14 Comparison of the strain and effective stress of three groups OPT compacted samples and the same water content uncompacted samples.....58

# 1. INTRODUCTION

Groundwater plays an important part in drinking water supply, geotechnical engineering practice and sustainable development (National Research Council, 1997; Todd and Mays, 2005). A variety of environmental pollutants may impair the use of water and raise concerns of public health (Todd and Mays, 2005). The contaminant resources of the ground water can be mainly divided into three categories: 1. Light Non-Aqueous Phase Liquids (LNAPLs), such as gasoline; 2. Dense Non-Aqueous Phase Liquids (DNAPLs), such as trichloroethylene (TCE) and perchloroethylene (PCE); 3. inorganics and other dissolved constituents, such as heavy metal cations,  $\text{Cr}^{6+}$ ,  $\text{As}^{3+}$ ,  $\text{Co}^{2+}$ ,  $\text{Cu}^{2+}$ ,  $\text{Zn}^{2+}$ ,  $\text{Mn}^{2+}$ , and etc. (National Research Council, 1997).

The traditional technology for the ground water remediation is the pump-and-treat method which is costly for operation and maintenance and needs energy consumption (United States Environmental Protection Agency, 1998). The permeable reactive barrier (PRB) is an alternative solution that exerts less influence on groundwater flow but also performs in-situ remediation. (Scherer *et al.*, 2000); It is also one of the economical methods to contain the contaminants in a complicated geological and hydrogeological conditions (Fronczyk and Garbulewski, 2013). The PRBs are in situ treatment zones capturing a plume of contaminants, confining the movement of contaminants and releasing the treated water (Gillham, 2010). For the past two decades the PRB raised great interest from scholars and engineering practitioners.

The reactive materials are the critical components of the PRB. The removal of contaminants from groundwater are typically achieved through: sorption and precipitation, chemical reactions and biological treatments (Tratnyek *et al.*, 2003). Zero-valent iron (ZVI) was the first and mainly used in PRB as the reactive material

for converting contaminants to nontoxic or immobile species, dehalogenating hydrocarbon sand precipitating anions and oxyanions for grounder water remediation, (United States Environmental Protection Agency, 1998; Scherer et al, 2000; Tratnyek et al, 2003; Gillham et al, 2010); Microorganisms or the material which stimulates the growth of microbes, such as humic materials and oxides, were commonly proposed as biological materials for PRB to remediate the nitrate and sulfate species (United States Environmental Protection Agency, 1998; Scherer et al, 2000); Zeolite was another ideal alternative material for PRB based on its adsorption capacity and high ion exchange capacities (Jorgensen and Weatherley, 2003; Altare et al, 2007; Fronczyk, 2008; Belbase et al, 2013; Joanna et al, 2013).

Zeolites are crystalline aluminosilicates with a three-dimensional framework structures (Dyer, 1988). They were initially named by a Swedish mineralogist due to its intumescence property (Cronstedt, 1756). Based on its molecular dimensional structures the zeolite has unique properties such as the high ion exchangeability, sorption capacity and shape selectivity (McCusker and Baerlocher, 2001). Depending on the ability of interacting with a variety of aqueous species, zeolites are not only ideal materials for ion-exchange beds during waste water treatment (Altare, 2007; Lv et al, 2014) but also excellent sorbents for environmental pollutants (Kayabali, 1997; Park et al, 2002; Tuncan et al., 2003; Ören and Kaya, 2013). Zeolites can be thermally regenerated without a significant decrease of adsorptive capacity (Li et al, 2014) so this allows zeolites to be used as near-ininitely as a cost-effective materials for PRB. A pilot-scale demonstration project near Portland, OR, indicated that the PRB, with a surfactant-modified zeolite as the reactive media, performed well for removing the chromate ( $\text{Cr}^{6+}$ ) and perchloroethylene (PCE) (Kovalick, 1999).

There are many kinds of natural and synthetic zeolites. The most common natural zeolite minerals clinoptilolite, chabazite, philipsite and mordenite (Birsoy, 2002; Ören and Özdamar, 2013) basically had the similar molecular structures (Dyer, 1988). By ion-exchanging the zeolite can remove cationic metals (e.g. Cu, Ni, Zn), Chromium and Perchlorate. And the clinoptilolite as a common natural zeolite (Ören and Özdamar, 2013) was rich of the alkali metal (sodium and potassium) (Dyer, 1988;

Mumpton, 1999) with honeycomb-like channels structure (Meier and Olson, 1978). Due to rich of alkali metal the clinoptilolite had ammonia removal ability from wastewater by ion exchanging process (Hlavay et al, 1982; Jorgensen and Weatherley, 2003; Du et al, 2005). Since the three-dimensional framework of  $[\text{SiO}_4]^{4-}$  and  $[\text{AlO}_4]^{5-}$  with the unique crystal structure the clinoptilolite had considerable channels (Alan Dyer, 1988; Ören, 2013). The reabsorbed water molecules and easy removable cations associated inside the channels (Alan Dyer, 1988) which gave the clinoptilolite relative high specific surface area, water holding capacity and ion exchange properties.

In addition to the application of sorbent/reactive material in PRB, zeolites were also recommended to be used as liner amendment materials (Ören et al, 2011) and backfilling additives (Hong, 2012). It was demonstrated by previous studies that when a rather low percentage of zeolite was added to liner or filling materials like bentonite or compacted clays, the contaminant retention and containment capacity of the multi-media can be significantly increased.

This study was motivated by applications of zeolites as reactive filter materials in reactive barriers, liners and fillings materials. And sand was chosen as the coarse grain to be combined with zeolite. Normally the sand control the stiffness and compressibility and the zeolite control the permeability of the mixtures (Kleppe and Olson 1985; O'Sadnick et al. 1995; Alston et al. 1997; Tay et al. 2001). When zeolites are combined with sands, hydraulic performance, deformational behavior and chemical activity of the mixtures are of critical importance to the design work. Take the permeable reactive barrier for instance, the keys for a successful application at the field is to ensure that 1. Hydraulic conductivity of the PRB materials (e.g. sand and zeolite) should be large enough for the conduction of groundwater flow; 2. The reactive material must be abundant such that the interaction with the contaminants can progress effectively. The relationship between the purposed PRB thickness and the hydraulic conductivity of the reactive materials could be calculated (Czurda and Haus 2002).

Soil compaction is the most effective and cost-efficient way to enhance the soil stability and lower the hydraulic conductivity and compressibility (Holtz and Kovacs,



1981). The effect of the compaction effort on the sand and zeolite mixtures merits examination for the field applications.

Some scholars had investigate the geotechnical behaviors of the zeolites or zeolite amended soil mixtures (Park et al, 2002; Lee et al, 2010; Ören et al, 2011; Ören and Ozdamar, 2013). Ören (2013) indicated that the maximum dry densities of the compacted zeolites were between  $1.01 \times 10^3 \text{ kg/m}^3$  and  $1.17 \times 10^3 \text{ kg/m}^3$ , the optimum water content (OPT) range was 38% to 53% and the hydraulic conductivity was  $2.0 \times 10^{-3} \text{ cm/s}$  to  $1.1 \times 10^{-7} \text{ cm/s}$ . And the effects of different compaction water contents on the zeolite compaction and hydraulic conductivity behavior were also investigated. From his study it was noted that both the particles size distribution and the compaction water content would influence the compaction and hydraulic conductivity behavior of the compacted samples.

There were also previous laboratory investigations on geotechnical behaviors for the uncompacted or slightly compacted zeolite (Park et al, 2002; Lee et al., 2010; Villarreal, 2013). It was noticed that compaction effort could significantly alter the density, voids distribution and swelling tendency of zeolite (Aksoy, 2010; Ören, 2013). But only few studies focused on the hydraulic conductivities of compacted zeolite (Ören, 2013) and compacted zeolite-bentonite mixtures (Kayabali, 1997; Ören, 2011). Little information is available on geotechnical engineering properties of the sand/zeolite mixtures. One important reason for the limited investigations of the geotechnical behaviors of the sand-zeolite is that most tests are time consuming. In addition, it's very difficult, if not impossible, to compare results from samples with varying zeolite contents and with different mineral types. So this study performed tests on both compacted and uncompacted sand and zeolite mixtures with controlled zeolite content.

In this study three ASTM standard tests were conducted to investigate the compaction, hydraulic conductivity and consolidation behaviors of the sand and zeolite (clinoptilolite) mixtures. The impact of the compaction and the zeolite content on the engineering properties of sand-zeolite mixtures were investigated and analyzed. Three different mass ratio groups (group one: 25% zeolite; group two: 50% zeolite;

group three: 75% zeolite) were used to investigate the compaction behaviors by the Proctor method. The hydraulic conductivity test using tap water was conducted in a rigid wall mold by the constant head and falling head method. Group 1 (25% zeolite) was used compacted samples to investigate the changing trend of the hydraulic conductivity with different compaction water contents. The hydraulic conductivity test for group 1 was conducted after the each compaction step in the rigid mold. The compacted samples with the optimum water content (OPT) of all the three groups and the uncompacted samples with the same water content of the each corresponding compacted sample OPT were used to investigate the effect of compaction and zeolite content on the hydraulic conductivity behaviors. One-dimensional consolidation test was used to test the consolidation behavior using the compacted samples with the OPT and uncompacted samples with the same water content of OPT. The compression index ( $C_c$ ), recompression index ( $C_r$ ), modulus of volume compressibility ( $m_v$ ) and the coefficients of consolidation ( $C_v$ ) were calculated for all the tested samples. The compaction and zeolite content on the consolidation behaviors were investigated.

## 2. MATERIALS AND METHODS

### 2.1 Materials

Three different mixtures of ASTM 20-30 sand and zeolite with varying mass ratios were used for the lab test. The specific gravity of the ASTM 20-30 sand was 2.67 and the zeolite was 2.33, as determined by ASTM D854-10 standard method in the lab, respectively. The pre-determined mass ratio was shown in the table 2.1. And the specific gravities of the sand and zeolite mixtures were calculated as the weighted average value of each material.

Table 2.1 Specific Gravity of sand-zeolite mixture

<b>Mass ratio</b>	<b>Specific gravity</b>
Group 1(75% sand &. 25% zeolite)	2.585
Group 2(50% sand &. 50% zeolite)	2.5
Group 3 (25% sand &. 75% zeolite)	2.415

#### 2.1.1 Zeolite

Zeolites are a well-defined class of crystalline naturally occurring aluminosilicates minerals. Four types of zeolite minerals (clinoptilolite, chabazite, mordenite and phillipsite) are typically most available due to both the abundant occurrence in nature and the ideal chemical activities (Jacobs and Förstner, 1999). The clinoptilolite was chosen for this study since its common occurrence in nature, strong exchange affinity for ammonia ( $\text{NH}_4^+$ ) and relatively strong cation exchange capacity

(Hedström, 2006; Hong and Shackelford, 2012; Li et al, 2014) comparing with other zeolite minerals.



Figure 2.1 The Zeolite powders  
(clinoptilolite, multavita Co.)

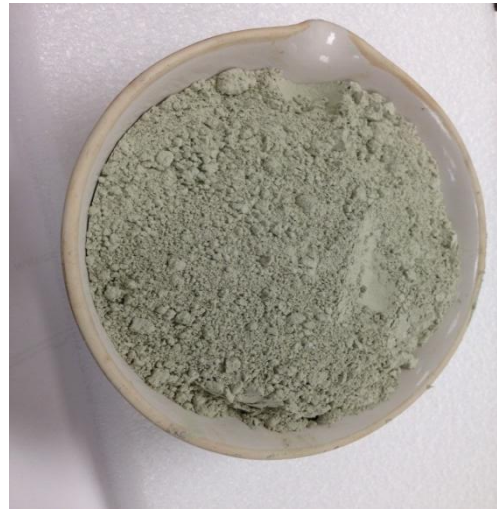


Figure 2.2 Zeolite for the tests

The Clinoptilolite chosen for this study was commercial fine powders (*figure 2.1*) with the chemical formula of  $[(Na,K,Ca)_{2-3}Al_3(Al,Si)_2Si_{13}O_{36} \cdot 12H_2O]$  (provided by *multavita Co.*). The bulk density of zeolite sample was  $880 \text{ kg/m}^3 \sim 960 \text{ kg/m}^3$  ( $55 \sim 60 \text{ lb/ft}^3$ , provided by *multavita Co.*). Due to its porous structure the density of zeolite was significant lower than the nature soil. The natural water content of the zeolite powders was about 5%.

The particle size distribution of zeolite was tested by ASTM422-07 and plotted in *figure 2.3*. According to the Unified Soil Classification System (USCS), the zeolite was classified as poorly graded silty sand.

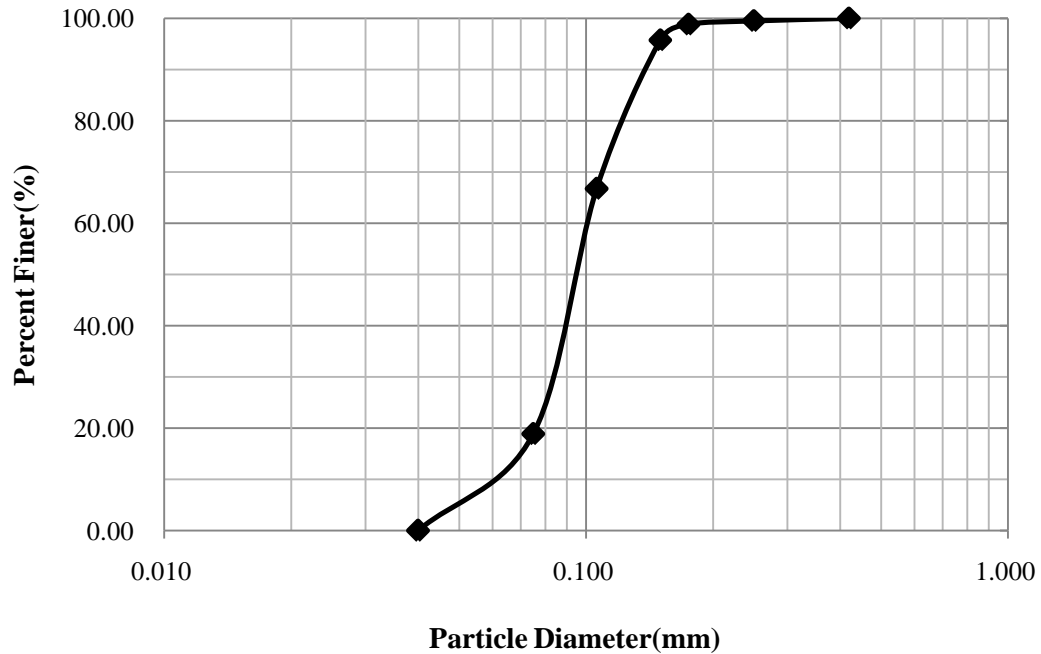


Figure 2.3 The particle size distributions of the lab zeolite (clinoptilolite)

### 2.1.2 ASTM 20-30 sand

The sand was a common test sand derived from natural Ottawa silica sand that passing the No.20 sieve (0.85 mm) and retained on a No.30 sieve(0.6mm) to the ASTM standard C778.The lab sand had a very low water content (lower than 0.1%) and more than 99% content was silica. The constituent grains of those sands were uncrushed and of rounded form (ASTM C77).

The tested ASTM 20-30 sand (figure 2.5) had a specific gravity 2.65(provided by supplier,2.67 from test). According to the Unified Soil Classification System (USCS), the ASTM 20-30 sand was poorly graded medium sand. The particle size distribution (figure 2.6) was tested by ASTM422-07 method and the specific gravity was tested by ASTM4318-10 method.



Figure 2.4 ASTM20-30 sand



Figure 2.5 ASTM20-30 sand particles (Nouvelle du Littoral Co).

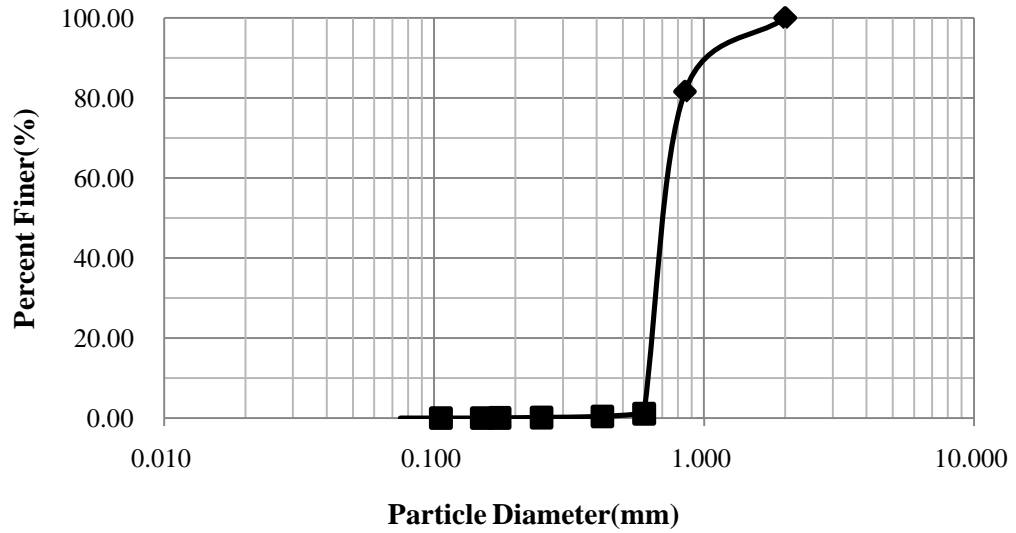


Figure 2.6 The particle size distributions of the lab ASTM20-30 sand

Table 2.2 Physical characteristics of sand and zeolite particles

	<b>Zeolite(clinoptilolite)</b>	<b>ASTM 20-30 sand</b>
Sand size fraction(%) [2-0.075mm]	81.1	100
Silt size fraction(%) [0.075-0.002mm]	18.9	0
Coefficient of uniformity, $C_u$	1.33	1.22
Coefficient of curvature, $C_c$	0.85	0.98
Specific gravity, $G_s$	2.33	2.67

## 2.2 Test methods

### 2.2.1 Lab tests arrangement

Three groups of the ASTM 20-30 sand and zeolite mixtures with pre-determined different mass ratios were used for the compaction (Proctor method) test. All the seven compacted samples with different water content in group 1 (25% zeolite) were performed the hydraulic conductivity tests in the rigid mold assembly after compaction. The compacted samples with the optimum water content (OPT) of the three groups and uncompact samples with the same water content were also tested for the hydraulic conductivities. And the one-dimensional consolidation tests were performed with three groups compacted and uncompact samples at OPT.

Table 2.3 Testing matrix

<b>Methods</b>		<b>Test name</b>		
		<b>Compaction ASTM 698-07</b>	<b>Hydraulic Conductivity ASTM 5856-07</b>	<b>Consolidation ASTM 2435-04</b>
<b>Materials</b>				
<b>Group 1</b>	<b>75% sand</b>	7	7samples C with different	2 samples
	<b>25% zeolite</b>	Samples	water contents and 1sample U with same OPT	C & U at OPT
<b>Group 2</b>	<b>50% sand</b>	6	2 samples	2 samples
	<b>50% zeolite</b>	Samples	C & U at OPT	C & U at OPT
<b>Group 3</b>	<b>25% sand</b>	6	2 samples	2 samples
	<b>75% zeolite</b>	Samples	C & U at OPT	C & U at OPT

\*The C stands for the compacted, U stands for the uncompacted and OPT stands for the optimum water content in the tests matrix below.

The *table 2.3* indicated that three ASTM standard methods were used to investigate the characteristics of the sand and zeolite mixtures. The samples numbers were listed and the corresponding results were shown in Chapter 3.

### 2. 2. 2 Particle size distribution and specific gravity test

The ASTM D854-10 standard method was used to determine the specific gravity of the ASTM 20-30 sand and the zeolite. The ASTM 422-07 standard method was used to test the particle size distributions of the sand and zeolite.

The zeolite powders with an initial water content approximate 5% was previously dried in the oven and then crumbed into small particles to yield a precise grain size distribution curve.



Table 2.4 Sieves selected in the particle distribution test

Sieve name	Sieve size (mm)
No.10	2.000
No.20	0.850
No.30	0.600
No.40	0.420
No.60	0.250
No.80	0.175
No.100	0.150
No.140	0.106
No.200	0.075
Pan	-

Nine sieves (table2.4)were selected to conduct the test. 300grams of oven dry test materials (both zeolites and ASTM 20-30 sand respectively) were shaken as long as all the particles could pass through sieve openings. The particles retained on each sieve were weighted. The percentage of the particles finer than each sieve was calculated and the particle distribution curves were plotted.

## 2.2. 3 Compaction tests

### 2.2.3.1 Method overview

Standard proctor tests (ASTM D698-12) were conducted to quantify the compaction behavior of three soil mixtures (detailed information in “testing matrix” part). A series of pre-determined water content were chosen for the sand-zeolite mixtures and their water content was measured. The relationships between the water content and the dry unit weight for each sample were plotted based on a sufficient number of repeated tests. The peak value of the dry density was determined as the maximum dry unit weight of the sand-zeolite mixture and the corresponding water content was determined as optimum water content (OPT). The impact of zeolite-sand mass ratio was compared in the test results part.

### 2.2.3.2 Main apparatus

Mold Assembly — the mold was made of rigid metal and cylindrical in shape.

The average diameter of the mold was  $4.000 \pm 0.016$  in. ( $101.6 \pm 0.4$  mm), the height was  $4.854 \pm 0.018$  in. ( $116.4 \pm 0.5$ mm) and the volume was  $0.0333 \pm 0.0005$  ft<sup>3</sup> ( $994 \pm 14$ cm<sup>3</sup>). Rigid metal base plate and extension collar should be securely attached and easily detached from the mold. The height of the extension collar assembly was above the top of the mold of at least 2.0 in. (50.8 mm) including an upper section and a funnel at least a 0.75 in. (19.0 mm) straight section beneath it. The extension collar was aligned with the inside of the mold. The bottom of the centrally recessed area and the bottom of the base plate should be planar. Two porous stones were placed on the top and bottom of the compacted sample. And string was used to avoid the upper stone floatation.



*Figure 2.7 Compaction mold assembly*



*Figure 2.8 Manual rammer*

Manual Rammer— the rammer equipped with a guide sleeve should have sufficient clearance. Vent holes at each end of the sleeve guaranteed the free fall of the rammer shaft and head. The diameter of the vent hole was  $\frac{3}{8}$  in. (9.5 mm).

### 2.2.3.3 Testing procedures

#### Samples prepared for the compaction test

Three different mass ratio sand and zeolite mixture samples were used for the compaction test. Approximately 5lb commercial ASTM 20-30 sand and zeolite under

each mass ratio were dried in the drying oven respectively. As all the sand and zeolite particles were finer than No.4 sieve (4.75-mm), no sieving was carried out before mixing. The mass of tested sand and zeolite dry particles were measured precisely and the particles were put into a container for the next test.

#### Estimate the OPT

Additional 100 grams dry oven sand-zeolite mixtures were added 4% water content (water content equals the ratio of the water and the dry soil mass) initially and mixed adequately. After mixing the moist soil mixtures were squeezed, bent and had its cross section observed. When mixture can be squeezed into a lump that sticks together and was broken into two pieces when bent, the water content of the mixture was expected to be at optimum water content. It was also observed that at water content lower than optimum soil samples tended to crumble while other soil samples with water content higher than optimum tended to stick together in a cohesive mass. A 2% water content increment was added to the soil mixture and the procedures above were repeated until finding the approximate optimum water content.



*Figure 2.9* Precisely adding water



*Figure 2.10* Estimating the OPT value



*Figure 2.11* Equably adding water

#### Adding water to the dry samples

2300 grams (approximate 5lb) dry sand and zeolite mixtures sample were

placed in a dry pot, the water was measured as a certain content of the dry sample in a graduated cylinder and poured into the wash bottle. The sample was mixed smoothly while adding the water equably (see *figure 2.11*). After mixed the sample was restored in a plastic bag for more than 16 hours before the compaction procedure. At least 5 samples at each certain water content were tested for the OPT value decision. So two wet samples and two dry samples with varying water content were prepared for the compaction.

### Compaction

The ASTM D698-07 method A was used to compact the samples in three layers with approximately equal thickness. 25 blows were stricken at each layer with the first four blows located at the four positive orientations. The soil not compacted or extending the compacted surface adjacent to the mold at the first two layers was trimmed. After the third layer was compacted the soil which slightly exceeded into the collar within 1/4-in. (6-mm) was trimmed carefully to avoid disruption.

After each compaction procedure at one certain water content ( $w$ ), the sand and zeolite mixtures sample was jacked out of the mold by the sample extruder. A geo-knife was used to slice off a 5g sample from central part of the soil mixtures and weighted in a container. The container with the wet soil mixtures was then put into the oven. Weight of the container with the dry soil mixture was measured and used to calculate the water content.

The sand and zeolite mixtures sample were reused at each test step of the same mass ratio. After each compaction finished the sand and zeolite mixtures sample was extruded out of the mold and broken into small particles. The used mixtures sample was broken into small lumps and put into the oven. After fully dried the sample was crumbed into small particles gently by hammer or heavy roller sieved by the No.20 sieve and then repeated the procedures above until all the small particles could through the No.20 sieve and No.30 in order to release the residual energy in mixture

lumps as much as possible.

#### 2.2.3.4 Calculation

The dry density after testing the water content by oven was calculated as:

$$\rho_d = \frac{\rho_m}{1 + \frac{w}{100}}$$

where:

$\rho_d$  = dry density of compacted specimen, g/cm<sup>3</sup>,

w = water content, %, and

$\rho_m$  = moist density of compacted specimen, g/cm<sup>3</sup>.

The dry unit weight of the compacted specimen was calculated as:

$$\gamma_d = 9.807\rho_d \text{ in kN/m}^3$$

= dry unit weight of compacted

The ZAV line (assuming S=1) and the saturation degrees of the mixtures samples were calculated as:

$$\gamma_d = \frac{G_s \gamma_w}{1 + e} = \frac{G_s \gamma_d}{1 + \frac{wG_s}{S}}$$

where:

$\gamma_d$  = dry unit weight of compacted specimen,

$\gamma_w$  = unit weight of water, and

$G_s$  = specific gravity of compacted mixtures specimen,

w = water content, %, and

S = saturation degree.

## 2. 2. 4 Hydraulic conductivity tests

### 2.2.4.1 Method overview

The hydraulic conductivity ( $k$ ) was investigated in a rigid-wall compaction-mold permeameter and the ASTM standard D5856-07 method was used to conduct the test. The tested hydraulic conductivity ( $k$ ) was based on the unsaturated conditions since it was hard to fully saturate the tested sample under the applied hydraulic gradient. Tap water under standard atmospheric pressure and temperature 20°C (68°F) was used as the permeant fluid through the samples. In order to account for the ion exchange properties of natural zeolite neither deionized nor distilled water were used for the test.

The compacted 75% sand and 25% zeolite mixtures with different water content were tested for the hydraulic conductivities. The measured hydraulic conductivity ( $k$ ) values versus water content ( $w$ ) was plotted to find the how did the moisture affect the rate of fluid conduction in the samples. Constant head method was chosen for samples on the dry side (water content ( $w$ ) values of the compacted samples less than the OPT value) while falling head method was chosen for samples on the wet side (water content ( $w$ ) values of the compacted samples larger than the OPT value).

In addition, two sets of tests were conducted for both compacted and uncompact samples at OPT (for the mass ratio of 50% sand and 50% zeolite and 25% sand and 75% zeolite, respectively). The impact of zeolite percentage in the mixture on the measured hydraulic conductivity ( $k$ ) was also discussed based on the results.

#### 2.2.4.2 Apparatus

##### Falling head testing system

The falling head testing system following the ASTM D5856-07 standard method was shown in the *figure 2.10*. It was used for testing the hydraulic conductivity values for the wet side specimen in group one and the compacted OPT samples in group two and three.

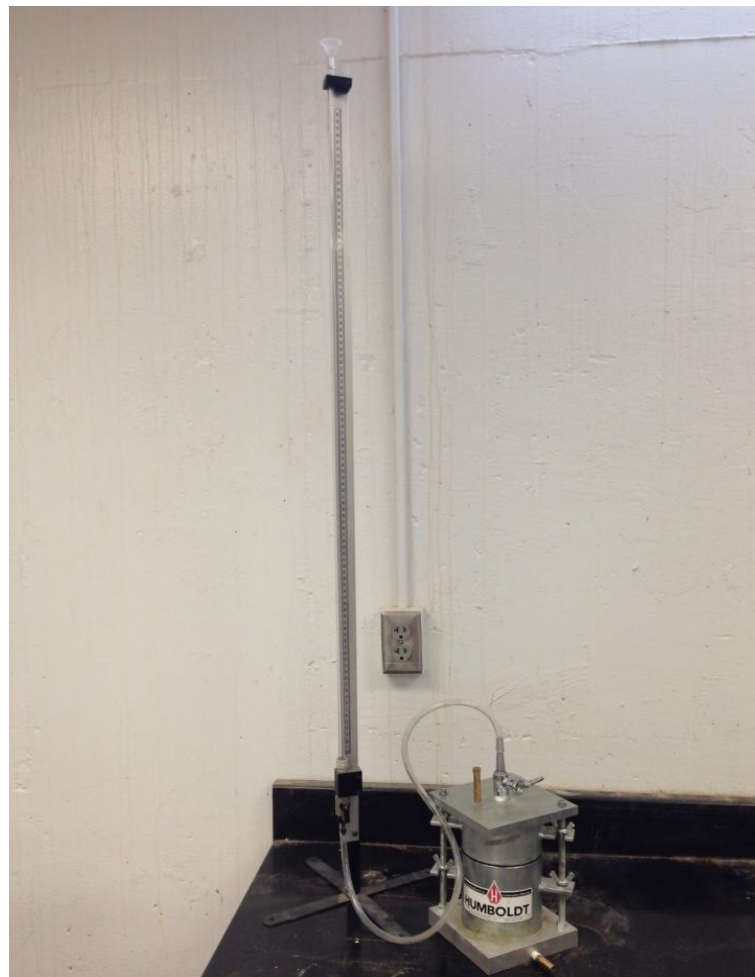


*Figure2.10 The falling head testing system*

## Constant head testing system

The constant head method was chosen for testing the hydraulic conductivity values for the specimen in group one on the dry side and the uncompacted samples both in group two and three. A big hand wash bottle was used to keep adding water to the top funnel to maintain a constant head for the test (see *figure 2.11*).



*Figure2.11 The constant head testing system*



#### 2.2.4.3 Testing procedures

##### Avoid the head lost in the mold assembly system

The mold assembly was assembled with porous discs and filter papers without a compacted specimen previously and tested the inflow and outflow to make sure that the hydraulic impedance was negligible. This was because although the most of the fine zeolite particles drainage can be avoided by the filter paper there were still some zeolite particles washed by the effluent flow clogging the bottom porous disc. So it was essential to check the head lost before each test.

##### Constant head method

The constant head method was conducted for testing the hydraulic conductivity of samples of the compacted and uncompact specimen with their water content lower than OPT. The specimen was prepared in the mold first and the testing steps followed the ASTM D5856-07 test method A. During the tests the ratio of outflow to inflow rate was maintained between 0.75 and 1.25. The specimen was permeated with water until at least four consecutive steady readings were obtained over a certain time interval. The applied hydraulic gradient was 9.52 for all the testing samples. Typically the hydraulic conductivity values were considered consistent if four or more consecutive hydraulic conductivity determinations fall within  $\pm 25\%$  of the mean value for  $k \geq 1 \times 10^{-10}$  m/s (ASTM D5856-07), and the hydraulic conductivity values of sand and zeolite mixtures were usually larger than  $1 \times 10^{-9}$  m/s (Ören, 2013).

##### Falling head method

The falling head method was used to test the hydraulic conductivity of the wet side samples in group1 and the compacted samples with OPT in group 2 and 3. Similarly a compaction sample was made in the rigid wall mold at certain pre-determined water content. And the mold assembly was connected for the falling head testing following the ASTM 5856-07 standard method. The applying hydraulic

gradient was smaller than 10 for all the testing samples. The high vacuum grease was used outside the junctions of the mold assembly to avoid leakage.

The falling head method was usually recommended for testing the samples with relatively small hydraulic conductivities. According to previous experience, it was expected that for the same sample, obtained results from falling head test would be slightly different from results from constant-head test.

Tap water (20°C) was used for the test which was inflated from the top vent port and a plastic string was used for sealing the top vent until no air bubble coming out from the influent port to the tube. The same standards as the constant head method were used to obtain at least four consecutive hydraulic conductivity values.

#### 2.2.4.4 Calculation

The total volume of the test specimen (V) from the length (H) and diameter (D) of the test specimen were calculated as:

$$V = \frac{\pi D^2 L}{4}$$

V = volume of the test specimen, m<sup>2</sup>,

L = length of the specimen, m,

D = diameter of the specimen, m<sup>2</sup>,

The hydraulic conductivity as the constant head method was calculated as:

$$k = \frac{VL}{Ath}$$

where:

k = hydraulic conductivity, m/s,

V = quantity of flow, taken as the average of inflow and outflow, m<sup>3</sup>,

L = length of specimen along path of flow, m,

A = cross-sectional area of specimen, m<sup>2</sup>,

t = interval of time, s, over which the flow Q occurs, and

h = difference in hydraulic head across the specimen, m of water.

The hydraulic conductivity as the constant head method was calculated as:

$$k = \frac{aL}{At} \ln\left(\frac{h_1}{h_2}\right)$$

where:

a = cross-sectional area of the reservoir containing the influent liquid, m<sup>2</sup>,

L = length of the specimen, m,

A = cross-sectional area of the specimen, m<sup>2</sup>,

t = elapsed time between determination of h<sub>1</sub> and h<sub>2</sub>, s,

h<sub>1</sub> = head loss across the specimen, at time t<sub>1</sub>, m, and

h<sub>2</sub> = head loss across the specimen at time t<sub>2</sub>, m.

## 2.2. 5 Consolidation tests

### 2.2.5.1 Method overview

Consolidation tests were performed for three groups of compacted and uncompact sand/zeolite mixtures with different zeolite percentage. The initial void ratio was determined and samples were saturated in the consolidometer before the test. The vertical load increment was doubled every 24 hours and the vertical displacement of the specimen height was measured according to certain time intervals. Once the maximum vertical stress (Typically 1089.81 kPa, stress produced by the 32kg, the total mass of the adding weight, 1kg converted to stress was approximate 34kPa in this test) was reached, the vertical load was removed and the unloading followed a reverse path of loading. Final void ratio was calculated at the end of each load step.

After finishing the unloading procedure a curve on a logarithmic axis was plotted to show the relationship between the effective stress and void ratio. The coefficient of consolidation was determined for evaluating the rate at which consolidation occurred. The secondary compression index for the recompression portion ( $C_r$ ) and the compression index for the virgin consolidation portion ( $C_c$ ) were determined from the compaction curve (ASTM D2435-04). The influence of the compaction on the compressibility of samples with optimum water content was evaluated by the comparison tests.

### 2.2.5.2 Apparatus

#### Consolidometer

A device to hold the testing sample in a rigid stainless steel ring with two porous disks on the each face of the sample was used to test the consolidation behavior. The inside diameter was measured by the vernier caliper with a tolerance of 0.075mm (0.003 in.). The testing sample was submerged in the device and the concentric vertical load was transmitted from the top porous disk. Negligible hydraulic

impedance filter paper was used on both side of the sample to avoid zeolite drainage when squeezing out the void space water during the consolidation.



Figure 2.12 The consolidometer

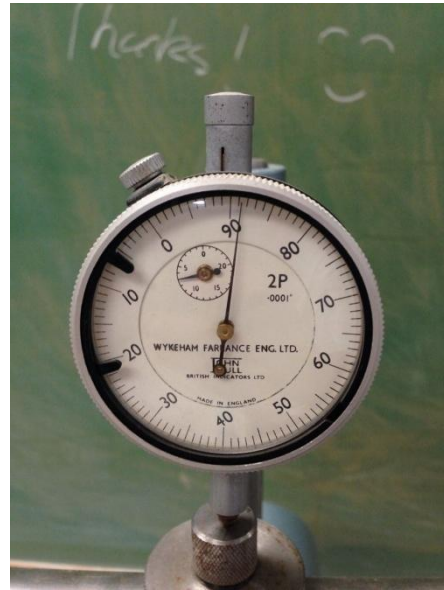


Figure 2.13 Deformation indicator

#### Deformation indicator

A sensitive deformation indicator with a readability of 0.0025 mm (0.0001 in.) was used to measure the displacement of the testing sample. The connecting beam was carefully locked to avoid additional deformation after placing the testing sample on the consolidation apparatus.

#### 2.2.5.3 Testing procedures

##### Specimen preparation

Three different mass ratio comparing specimen (compacted and uncompacted) at the OPT were prepared for the consolidation tests. The compacted specimen was made like *figure 2.14* and uncompacted specimen was slightly condensed into the ring just to avoid spill out.



Figure 2.14 Compacted specimen



Figure 2.15 Filter paper for consolidation

### Consolidation

Following the ASTM D2435-04 Standard method the consolidation tests were performed in 24 hour load increments and the vertical load was doubled every 24 hours. Six load steps were applied for the test and the first step load was 34.06 kPa. Measure the vertical displacement corresponding to each standard time intervals:

Table 2.5 Loading and unloading procedures of the consolidation test

Loading					
Day 1	Day 2	Day 3	Day 4	Day 5	Day 6
34.06 kPa	68.11 kPa	136.23 kPa	272.45 kPa	544.91 kPa	1089.81 kPa
Unloading					
Day 7	Day 8	Day 9	Day 10	Day 11	Day 12
544.91 kPa	272.45 kPa	136.23 kPa	68.11 kPa	34.06 kPa	0 kPa

#### 2.2.5.4 Calculation

Compression index and recompression index were calculated as:

$$C_c = -\frac{e_2 - e_1}{\log \frac{\sigma_2}{\sigma_1}} \quad C_r = -\frac{e_2 - e_1}{\log \frac{\sigma_2}{\sigma_1}}$$

where:

$C_c$  = Compression index,

$C_r$  = Recompression index,

$e_{1,2}$  = Void ratio, no units, and

$\sigma_{1,2}$  = Effective stress, kPa.

The modulus of volume compressibility was calculated as:

$$m_v = -\frac{\varepsilon_2 - \varepsilon_1}{\sigma_2 - \sigma_1}$$

where:

$m_v$  = modulus of volume compressibility,  $\frac{m^2}{kN}$ ,

$\varepsilon_{1,2}$  = Vertical strain, no units, and

$\sigma_{1,2}$  = Effective stress corresponding to the certain void ratio, kPa.

The volume of the solid was calculated as:

$$V_s = \frac{M_d}{G_s \rho_w}$$

where:

$G_s$  = specific gravity of the solids, unitless,

$\rho_w$  = density of water,  $1.0 \text{ g/cm}^3$ ,

$V_s$  = volume of the solid,  $\text{cm}^3$ , and

$M_d$  = mass of dry soil, grams.

The height of the solid was calculated as:

$$H_s = \frac{V_s}{A}$$

where:

A = specimen area, cm<sup>2</sup> or m<sup>2</sup>, and

H<sub>s</sub> = Height of the solid, cm or m.

The void ratio before and after test was calculated as:

$$\text{Void ratio before test: } e_0 = \frac{H_0 - H_s}{H_s}$$

$$\text{Void ratio after test: } e_f = \frac{H_f - H_s}{H_s}$$

where:

H<sub>0</sub> = initial specimen height, cm or m, and

H<sub>f</sub> = final specimen height, cm or m.

The coefficient of consolidation was calculated as:

$$c_v = \frac{TH_{dr}^2}{t_{90}}$$

where:

T = a dimensionless time factor, use 90% consolidation with T = T<sub>90</sub> = 0.848,

t<sub>90</sub> = time corresponding to the 90% consolidation, s or min, and

H<sub>dr</sub> = length of the drainage path, cm or m.



### 3. RESULTS AND DISCUSSION

#### 3.1 Compaction

##### 3.1.1 Group 1 – 75% ASTM 20-30 sand and 25% zeolite

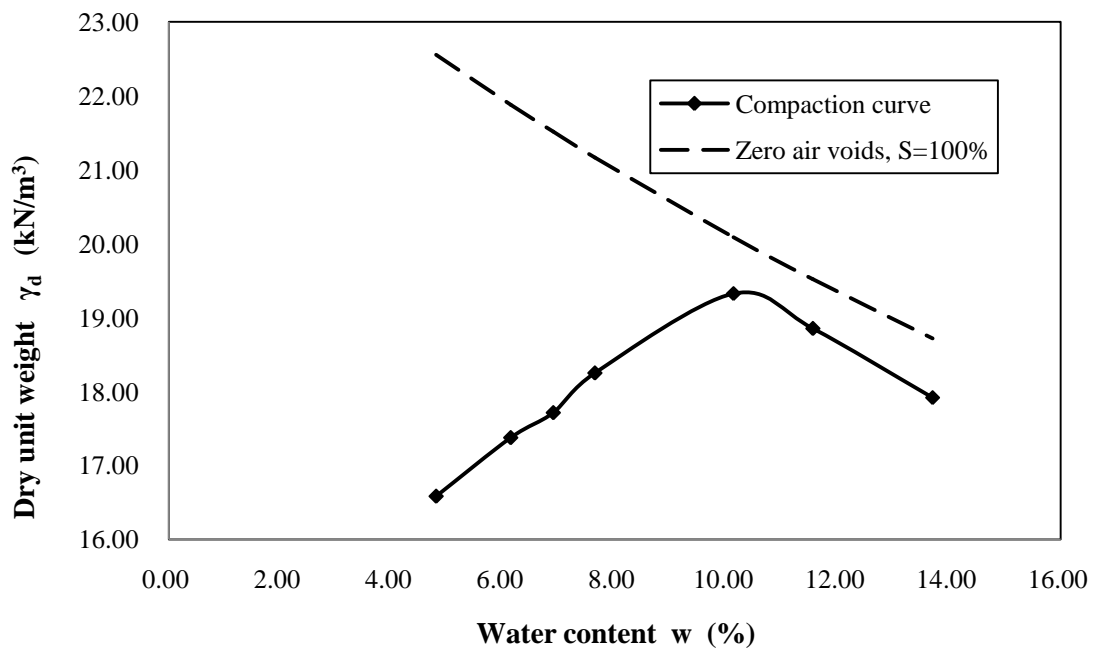


Figure 3.1 Compaction curve vs. different water content (75% sand and 25% zeolite)

The compaction results of dry unit weight vs. water content for the proctor test of the group 1 (75% ASTM 20-30 sand and 25% zeolite) sample were shown in Figure 3.1. Increment of water content (less than 4% as the recommendation of ASTM D698-07) was used for a series of samples. Initially, on the dry side of the compacted sample (water content smaller than the optimum water content), as the water content were increased the absorbed water film around the particles became thicker and the

particles were condensed more easily. A peak of dry density and water content was reached and, the corresponding water content was the optimum water content(OPT) and the dry unit weight was the maximum dry unit weight of the tested soil mixture, respectively. According to the curve the optimum water content(OPT) was 10.14% and the related maximum dried unit weight was  $19.33 \text{ kN/m}^3$ . After the OPT the lighter weight water would replace the heavier sand and zeolite mixtures particles and the dry unit weight tended to be decreased as the water content increased.

The Zero Air Void (ZAV) line represents the theoretical dry unit weight with zero air voids (100% saturation) and it's a theoretical line can't be reached by compaction curve no matter how large the compaction effort was applied. The degree of saturation (S) of the sand-zeolite mixtures sample at the optimum water content was calculated as 83.96%. The degree of saturation of samples on dry side of the OPT was typically much lower and the compaction curve was also far away from the ZAV line (see *figure 3.1*). Oppositely the degree of saturation of samples on the wet side was relative high and the compaction curve tends to be parallel to the ZAV line since the water occupied more space of the voids in the mixture samples.

The compaction curve was a hump shape which was typical for silty soils (Budhu, 2012). Capillary tension occurred in the sand particles after adding water to the mixture samples initially (Holtz, 1981; Budhu, 2012). So the compaction energy would overcome the capillary tension firstly and then re-organize the sample particles. And in group one 75% percent of the mixtures was the ASTM 20-30 sand so the compaction curve shape was identified more similarly to the common medium sand.

### 3.1.2 Group 2 – 50% ASTM 20-30 sand and 50% zeolite

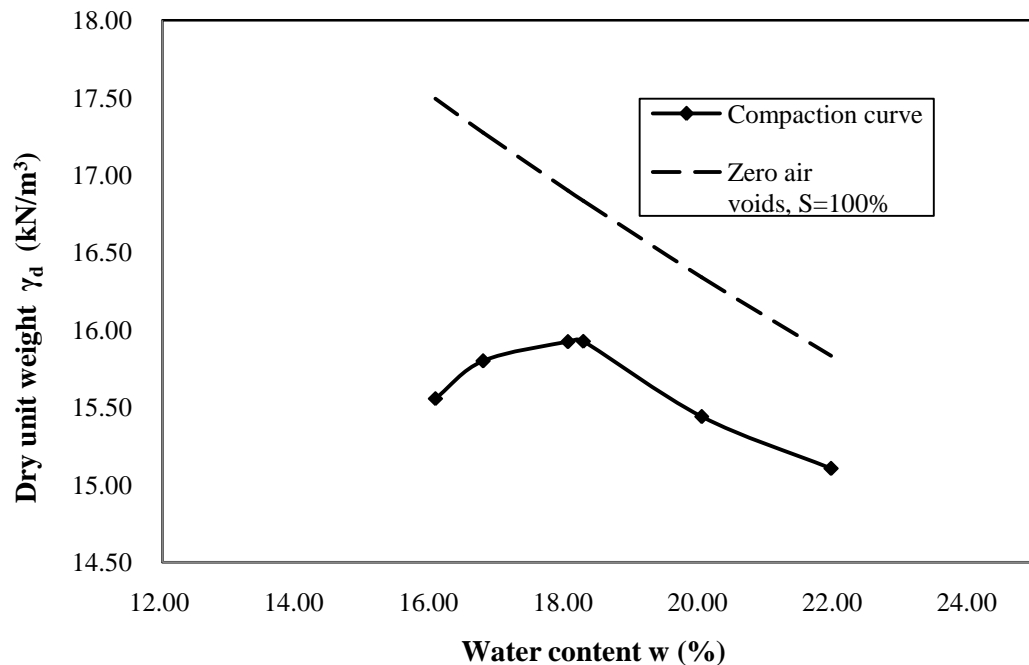


Figure 3.2 Compaction curve vs. different water content (50% sand and 50% zeolite)

Figure 3.2 indicated that the proctor compaction test results of group two (50% clinoptilolite). The optimum water content of the group two (50% ASTM 20-30 sand and 50% zeolite) was 18.26% which was about 8% larger than the group one. Also the maximum dry unit weight of the group two was 15.93 kN/m<sup>3</sup>, or 80% of maximum dry unit weight of group one. The degree of saturation at the optimum water content point was 84.04% just a little bit higher than the group one.

The compaction curve shape was not similar with either the medium sand or the fine particle soils. Both the ASTM 20-30 sand and the zeolite were the dominant particle groups in the mixture samples (50% respectively) and both of them affected the compaction behavior. So the shape was not as common as either the silt or the sand.

### 3.1.3 Group 3 – 25% ASTM 20-30 sand and 75% zeolite

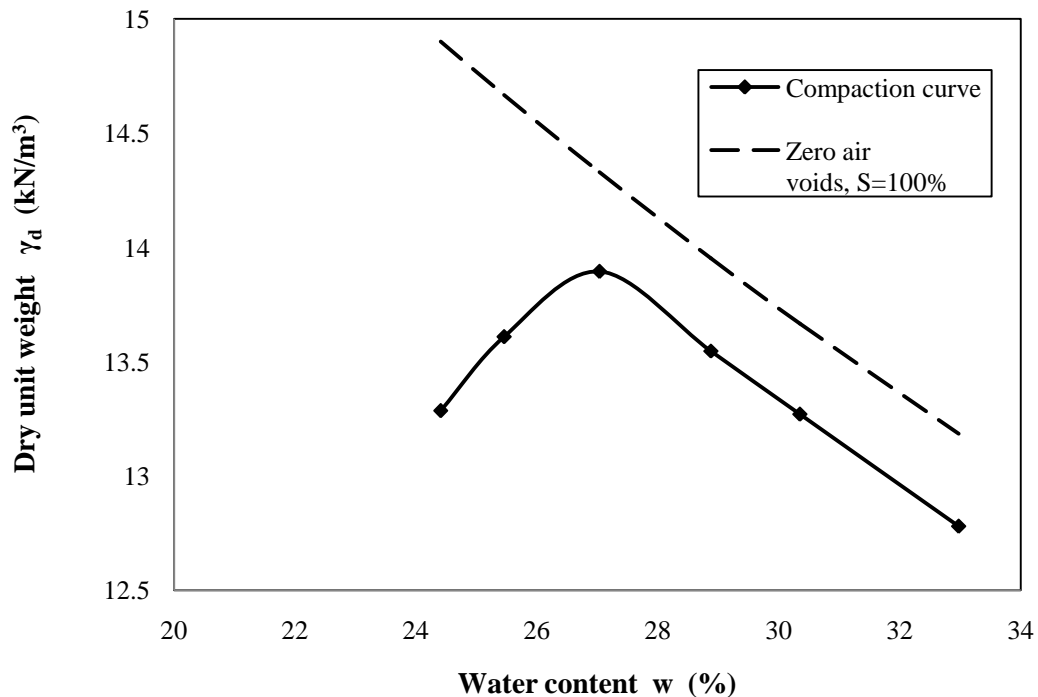


Figure 3.3 Compaction curve vs. different water content (25% sand vs. 75% zeolite)

Figure 3.3 indicated that the optimum water content of the group3 was 27.03% and the maximum dry unit weight was 13.89 kN/m<sup>3</sup>. The degree of saturation at the OPT was 93.16%. The curve shape was similar to the bell-shape which was the typical for silts and clays.

During the compaction tests, the rebound of rammer on moist samples, especially with the water contents around the OPT point, were observed. This phenomenon was also observed in group 2 and group3. And additional inputted energy were exerted on the samples due to this “second blow”. The extra blows inevitably added the exceeding energy to the specimen which also would shift the final compaction curve to the left-top hand side in the chart (see figure 3.4, Lambe, 1962). And the measured OPT value tended to lower than the actual value while the maximum dry unit weight was larger.

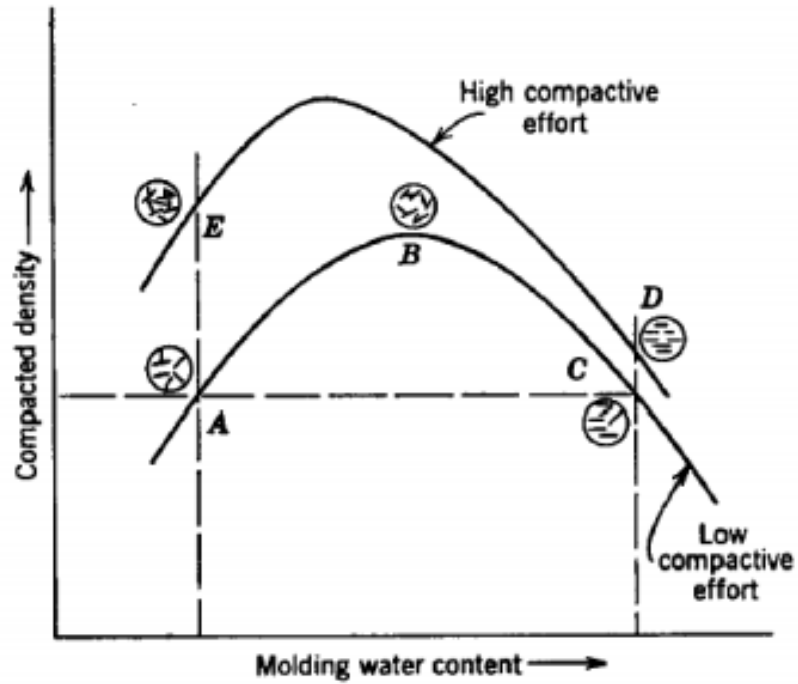


Figure 3.4 Effects of compaction on structure. (Lambe, 1962)

### 3.1.4 Comparison of three groups compaction test

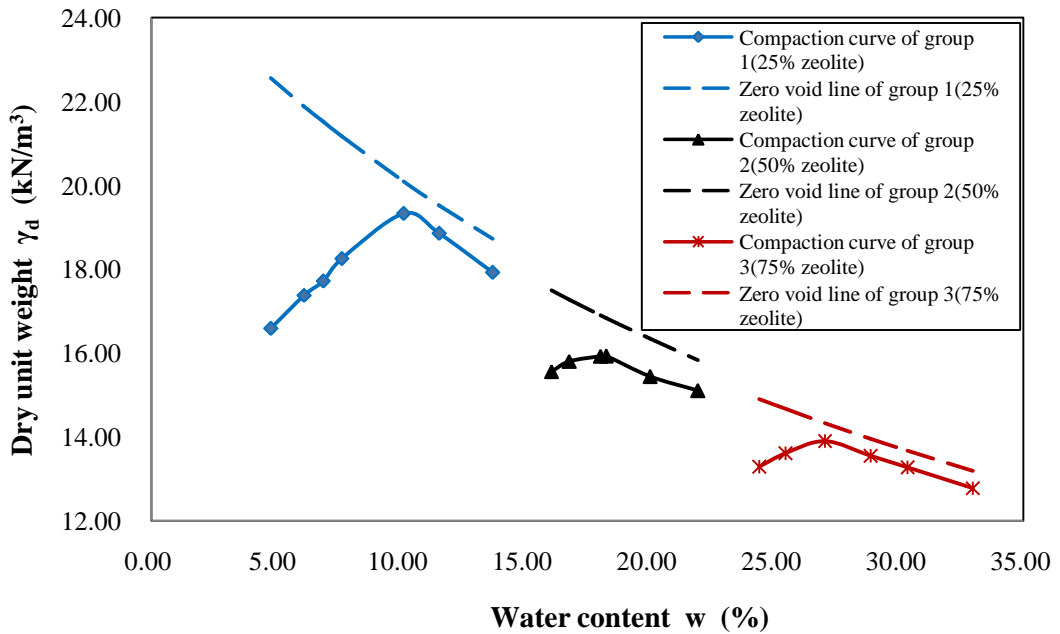


Figure 3.5 Comparisons of three groups compaction curves

The *figure 3.5* showed the comparison of the three groups of compaction curves. As the curves indicating the OPT values became larger as the zeolite percentage was increased.

Due to lack of the information from the *multavita Co.* the specific surface of the clinoptilolite was estimated as  $40 \text{ m}^2/\text{g}$  (Hong et al, 2012), which was significantly larger than the ASTM 20-30 sand with specific surface of  $0.007 \text{ m}^2/\text{g}$  (Lee et al, 2003). Consequently, compared with the ASTM 20-30 sand the zeolite particles had larger water holding capacity and more water was needed to saturate the zeolite-sand mixtures when percentage of zeolite increased (see table 3.1). For the compaction tests, more water was needed to lubricate the particle surfaces to reach the maximum dry unit weight as zeolite mass ratio of the mixtures samples was increased.

The lowered maximum dry unit weight of compacted samples with higher zeolite content could be attributed to the lower density of zeolite particles and higher water hold capacity of them. According to the *multavita Co.*, the bulk density of the zeolite used in this test was about  $880 \text{ kg/m}^3 \sim 960 \text{ kg/m}^3$  ( $55 \sim 60 \text{ lb/ft}^3$ ), which was obviously lower than the nature sand  $1570 \text{ kg/m}^3$ . And the specific gravity of the zeolite was 2.33 that was smaller than the sand (2.67). In addition, zeolite were finer particles with larger specific surfaces and consequently, the zeolite dominated mixtures needed more water to saturate the particle surface and facilitate the particle movement to reach a denser state. So adding more zeolite to the mixture sample for the compaction will result in the lower maximum dry unit weight at the optimum water content.

Table 3.1 Data acquisition of proctor compaction test results for three groups

Name	water content (%)	dry unit weight (kN/m <sup>3</sup> )	degree of saturation (%)
<b>group 1</b> <b>(25% zeolite &amp; 75% sand)</b>	4.80	16.58	23.45
	6.14	17.37	34.55
	6.90	17.71	41.37
	7.65	18.25	50.80
	<b>10.14(OPT)</b>	<b>19.33( Maximum)</b>	<b>84.04</b>
	11.56	18.85	86.68
	13.70	17.92	85.39
<b>group 2</b> <b>(50% zeolite &amp; 50% sand)</b>	16.06	15.56	69.71
	16.77	15.80	76.00
	18.03	15.92	83.52
	<b>18.26(OPT)</b>	<b>15.93( Maximum)</b>	<b>84.64</b>
	20.02	15.44	85.13
	21.94	15.11	88.04
<b>group3</b> <b>(75% zeolite &amp; 25% sand)</b>	24.41	13.29	75.31
	25.46	13.61	83.06
	<b>27.03(OPT)</b>	<b>13.89( Maximum)</b>	<b>92.67</b>
	28.88	13.55	93.20
	30.35	13.27	93.39
	32.97	12.78	93.32

The table 3.1 indicated the degrees of saturation for samples on the wet side of the OPT tended to be larger as the zeolite percentage of the increased. Since the zeolite had large water holding capacity more water was needed to saturate the surfaces of particles such that particles could be rearranged under compaction effort.

In the group2 and group3 the mass ratio of the fine particles zeolite was considerable. It was hard to totally break the reused fine particles structures to recover them to the initial state with the help of oven and sieves. From the energy point of view, breaking the reused mixtures samples and making sure them through the certain sieve can release the most part of the energy but there were still absorbed energy in the fine zeolite aggregates which can't be neglected when the mass ratio of zeolite was relatively high. The pre-absorbed excess energy by the last compaction will result the high compaction energy level comparing with the standard proctor test and shift the final compaction curve to the left-top hand side in the chart. And the optimum

water content obtained from the chart would be less than the actual value while the maximum dry unit weight would be larger.

To conclude, based on the same energy level of the compaction (Proctor compaction) when the zeolite mass ratio was increased the compaction curve would shift to the right-down hand side with the larger optimum water content and lower maximum dry unit weight.



## 3.2 Hydraulic conductivity

### 3.2.1 Hydraulic conductivity test for pre-compacted test samples with different water content of group1 – 75% ASTM 20-30 sand and 25% zeolite (clinoptilolite)

Group 1 (25% zeolite) was performed to investigate the different water contents impacting on the changing trend of the hydraulic conductivity behaviors of the compacted sand-zeolite mixtures samples. Constant head method was used for the pre-compacted samples with water content slower than the OPT while falling head method was performed for the samples with higher water contents.

The testing results of hydraulic conductivity ( $k$ ) at different water contents ( $w$ ) were summarized in table 3.2. The relationship between the hydraulic conductivity ( $k$ , in log scale) and the water content ( $w$ ) was plotted in the *figure 3.6*. The hydraulic conductivity  $k$  for a given water content was tested by at least three trials and the stand deviations of  $k$  were shown in the figure. The results for constant-head tests and falling-head tests were plotted with separate colors.

The effects of different water contents on the hydraulic conductivity behaviors of the compacted samples were briefly discussed in this part.

Table 3.2 The data acquisition of hydraulic conductivity test results for different water content of 75% ASTM 20-30 sand and 25% zeolite mixtures compacted sample

water content w (%)	dry density $\gamma_d$ (g/cm <sup>3</sup> )	hydraulic conductivity k (cm/s)	degree of saturation(%)	void ratio $e_0$
4.80	1.69	$2.75 \times 10^{-4}$	23.43	0.53
6.14	1.77	$2.59 \times 10^{-4}$	34.47	0.46
6.90	1.81	$1.95 \times 10^{-3}$	41.66	0.43
7.65	1.86	$7.12 \times 10^{-4}$	50.73	0.39
<b>10.14 (OPT)</b>	<b>1.97</b>	<b><math>2.05 \times 10^{-7}</math></b>	<b>83.96</b>	<b>0.31</b>
11.56	1.92	$6.58 \times 10^{-7}$	86.28	0.34
13.70	1.83	$1.13 \times 10^{-6}$	85.84	0.41

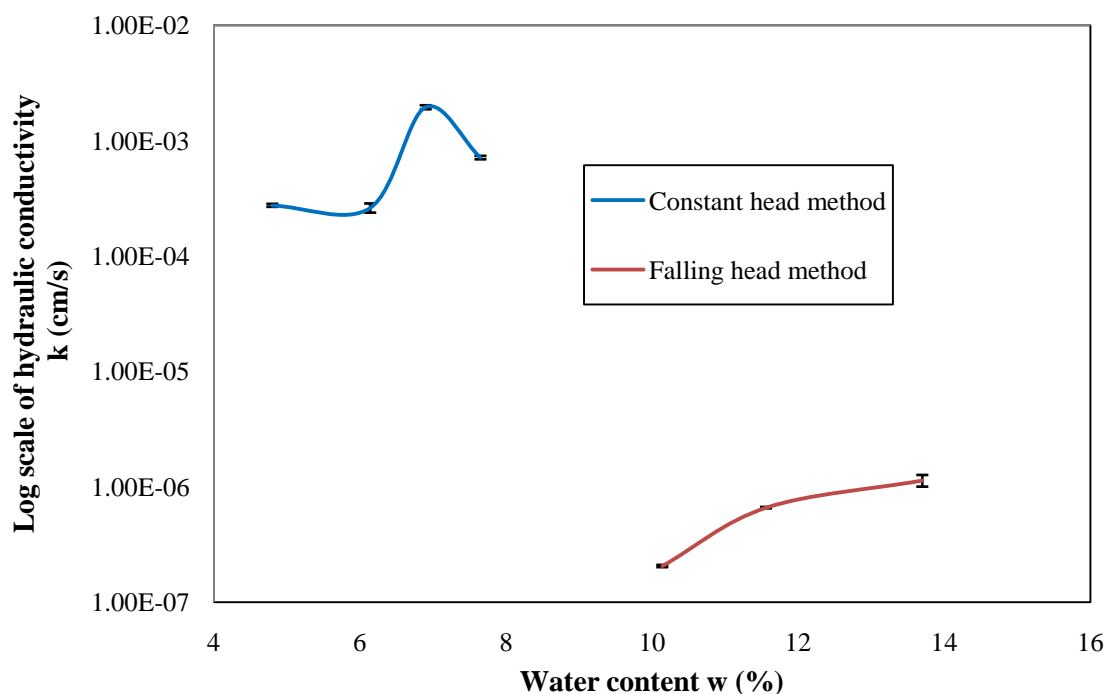


Figure 3.6 Log scale of hydraulic conductivity vs. different water content of 75% ASTM 20-30 sand and 25% zeolite mixtures compacted sample

Table 3.2 showed the tested hydraulic conductivity vs. different water content of the compacted group 1 (25% zeolite) samples. All testing samples were compacted previously and had their water content measured. On the dry side of the OPT, the range of the hydraulic conductivity were  $1.95 \times 10^{-3}$  cm/s to  $2.05 \times 10^{-7}$  cm/s, with the peak value occurring at water content of 6.9%. The measured maximum hydraulic conductivity was approximate 4 orders of magnitude larger than the hydraulic

conductivity at the optimum. It was observed that the measured hydraulic conductivities on the dry side of the OPT were very different from those on the wet side. At the wet side the hydraulic conductivity range was from  $1.13 \times 10^{-6}$  cm/s to  $2.05 \times 10^{-7}$  cm/s. The difference value at the wet side was approximately in one order of magnitude and the curve tended to level out. The compacted samples on the wet side had similar hydraulic conductivity behavior of compacted clay when comparing with the compaction-permeability tests on Siburua clay (Lambe, 1962).

There were several parameters could have impacted the hydraulic conductivity of tested samples. In this series of tests only the water content were chosen as the variable and studied. And the hydraulic conductivities of samples on the dry side (water content smaller than the OPT) were obviously larger than the ones of the wet side (water content larger than the OPT). As the table 3.2 showed on the dry side as the compaction water content increased the degree of saturation raised significantly. On the dry side the degree of saturation was relatively low and more air were possibly entrapped and stored in the void space of the mixture. Since the unsaturated hydraulic conductivities were tested in this test and the entrapped air bubbles were hardly forced out by the relatively small hydraulic gradient (less than 10), the entrapped air bubbles would decrease the effective void ratio and inevitably affect the tested value of the hydraulic conductivity. But it was hard to evaluate how much air was entrapped and the entrapped air would dramatically change the hydraulic conductivity value of the unsaturated sample (Todd, 2005). That might be the reason resulted in the peak tested value. But the degree of saturation tended to be equal on the wet side. The smallest hydraulic conductivity value appeared at the OPT point and the values tended to be a little larger as the compaction water content increased. It was noted that under the approximately same degrees of saturation the wet side void ratios tended to increase as the compaction water content increased. That might result in the increasing trend of hydraulic conductivity on the wet side.

For the compacted mixtures samples the relationship between the void ratio and hydraulic conductivity was far from linear (Bengochea et al, 1979). It was obvious that the void ratios of the compacted samples on the dry side were approximately

equal to values on the wet side but the tested values of hydraulic conductivities were dramatically different.

The previous compaction tests also prepared the tested sand- zeolite mixtures sample for the next step hydraulic conductivity tests in the rigid mold. Some capillaries were formed between the mixture particles due to the small void.

One possible shortcoming of this test method was the possibility that the water path would occur along the interface between the tested sample and the rigid compaction mold (ASTM5856-07). But the tested samples were compacted samples and the samples would swell in the mold when exposed to water (by observing after each hydraulic conductivity test, especially the samples with high zeolite content). So the leakage problem was negligible in this test.

### 3.2.2 Hydraulic conductivity test for both pre-compacted (OPT) and uncompacted (same water content) samples with different zeolite (clinoptilolite) content

These series of tests were performed to investigate the compaction effort and zeolite content on the measured hydraulic conductivity of sand-zeolite mixtures. Falling head method was conducted for the pre-compacted samples with the OPT and constant method was performed for the uncompacted samples with the same water contents of the OPT for each mass ratio. The applied hydraulic gradient was 9.52 for the constant head method and smaller than 10 for the falling head method. And a group of uncompacted pure sand was also tested for comparison.

Table 3.3 The data acquisition of hydraulic conductivity test results for both pre-compacted (OPT) and uncompacted (same water content of the OPT) test samples with different zeolite (clinoptilolite) content

Sample name	water content w (%)	hydraulic conductivity k (cm/s)	degree of saturation (%)	void ratio $e_0$
pure sand	0.00	$2.14 \times 10^{-2}$	0.00	0.72
uncompacted (25% zeolite)	10.14	$3.80 \times 10^{-3}$	26.69	0.98
uncompacted (50% zeolite)	18.26	$5.89 \times 10^{-4}$	33.52	1.18
uncompacted (75% zeolite)	27.03	$5.04 \times 10^{-5}$	47.57	1.37
compacted (25% zeolite)	10.14	$2.05 \times 10^{-7}$	84.04	0.31
compacted (50% zeolite)	18.26	$1.91 \times 10^{-7}$	84.64	0.54
compacted (75% zeolite)	27.03	$1.67 \times 10^{-7}$	92.67	0.70

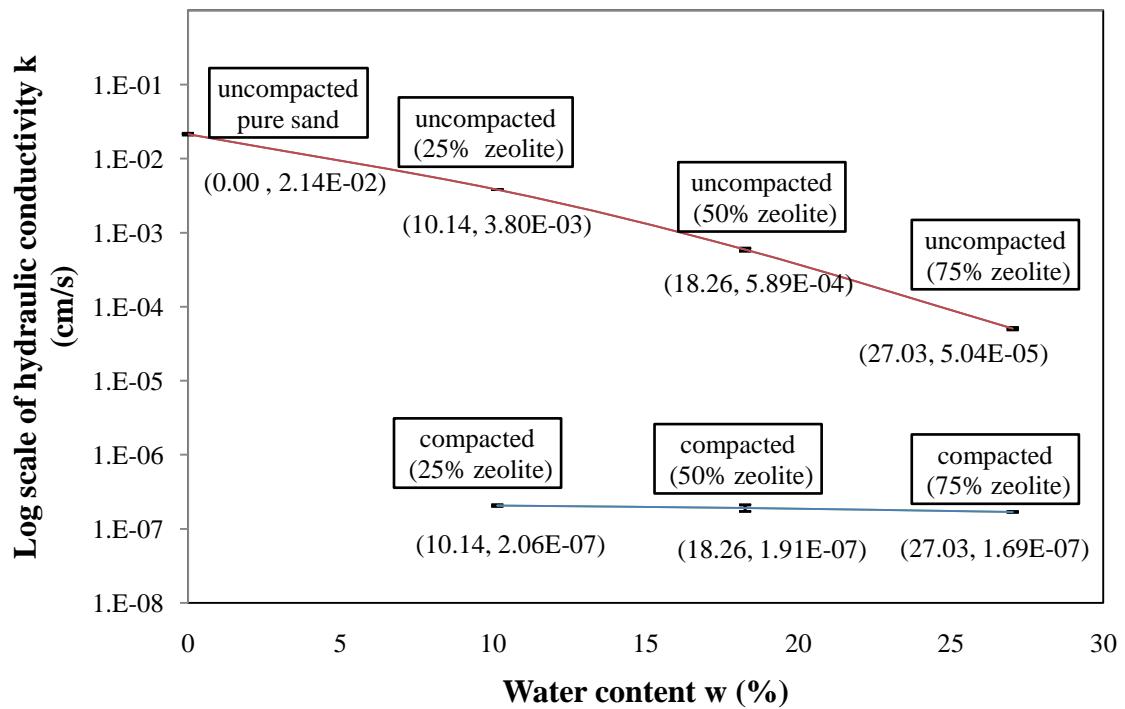


Figure 3.7 Log scale of hydraulic conductivities vs. different water content of all the three groups compacted and uncompacted samples and uncompacted pure ASTM 20-30 sand sample

The testing results of hydraulic conductivity ( $k$ ) at different water contents ( $w$ ) were summarized in table 3.3. The curve of the log scale of the hydraulic conductivity ( $k$ ) and the water content ( $w$ ) were plotted in the figure 3.7 including the stand

deviation of measured k results at different water content. As the two curves shown, for the uncompacted samples the hydraulic conductivities ranged from  $2.14 \times 10^{-2}$  cm/s to  $5.04 \times 10^{-5}$  cm/s while the hydraulic conductivities ranged from  $2.05 \times 10^{-7}$  cm/s to  $1.70 \times 10^{-7}$  cm/s for the compacted samples.

Table 3.3 indicated the tested hydraulic conductivity values of the uncompacted samples tended to be reduced approximately one order of magnitude while the zeolite (clinoptilolite) percentage increased 25% in the mixtures samples. It was noted that the zeolite percentage of the uncompacted mixtures had significant influence on the hydraulic conductivity behavior. This was attributed to the unique properties of zeolite. As introduced in the materials chapter the zeolite was porous material with very open frameworks, channels and cavities. When the zeolite dominated the mixtures sample the orientations of the open channels inside zeolite were random and the water path through the permeable media became complicated (see *figure 3.9*). Therefore the drag force to the permeant fluid could increase as finer zeolite particles increased. Also the zeolite had relatively larger specific surface area than the sand. So comparing with the ASTM 20-30 sand the zeolite particles had higher water holding capacity. The water molecule was easier to be enwrapped and fixed as a film by zeolite than the sand. And then the effective void ratio of the mixtures decreased resulting in lower hydraulic conductivity.

As the table 3.3 showed the void ratio of the uncompacted sample tended to be larger from pure sand to 75% zeolite. But as the zeolite content increased more water molecule was fixed and occupied the void space when the hydraulic conductivity test was performed. The effective void for the passing flow tended to be smaller and the hydraulic conductivity tested value tended to be lower. And in test if the effluent flow was not strong enough the time interval should be large enough to avoid the record error of operating the time locker. The applied hydraulic gradient was 9.52 and the water pressure would condense the uncompacted sample at the very beginning of the test and result in decreasing the initial hydraulic conductivity tested value.

When comparing the tested results between the compacted and uncompacted samples based on the same zeolite percentage, it was obvious that the compaction

effort would significantly decrease the hydraulic conductivity of zeolite/sand mixtures. The compaction effort decreased the hydraulic conductivity values about 4 orders of magnitude of the 25% zeolite mixtures while approximately 3000 times of the 50% zeolite mixtures and 300 times of the 75% zeolite mixtures. The void ratio of the 25% zeolite mixtures decreased from 0.98 to 0.31 (about 3 times) while 1.18 to 0.54 (about 2.2 times) of the 50% zeolite mixtures and 1.37 to 0.70 of the 75% zeolite mixtures (less than 2 times). As the zeolite percentage increasing in the mixtures, the compaction effort in terms of decreasing the void ratio was not significant like the mixtures with low percentage of zeolite. Since when the sand dominated the mixtures compaction effort forced the smaller zeolite particles to occupy the void space between the larger sand particles and rearranged the mixtures matrix (see *figure 3.8*). The void ratio reduced effectively. But when the zeolite dominated the mixtures, as discussed above, the zeolite itself contained inside void space and compaction effort hardly reduced the void ratio significantly.

However, for the three compacted samples with the OPT, the tested hydraulic conductivity values were basically in the same order of magnitude. It was noticed that the void ratios for the compacted samples were increased as the zeolite (clinoptilolite) mass ratio increased but the hydraulic conductivity values tended to be slightly reduced. This indicated that compaction effort had greater impact on the hydraulic conductivity of sand/zeolite mixtures other than zeolite content.



*Figure 3.8 Sand dominate the mixture matrix*([http://www.ux1.eiu.edu/~cfjps/1300/sed\\_rxs.html](http://www.ux1.eiu.edu/~cfjps/1300/sed_rxs.html))



*Figure 3.9 Zeolite dominate the mixture matrix*([http://www.ux1.eiu.edu/~cfjps/1300/sed\\_rxs.html](http://www.ux1.eiu.edu/~cfjps/1300/sed_rxs.html))



The hydraulic conductivity tests for the compacted samples were conducted by the falling head method. The initial hydraulic gradient was about 10 as recommended for the hydraulic conductivity range from  $1 \times 10^{-6}$  cm/s to  $1 \times 10^{-7}$  cm/s (ASTM D5856-07). Typically the hydraulic gradient from 1 to 5 covered most field conditions (ASTM D5856-07). The reason was that the high water pressure would consolidate the specimen, generate some channeling around the inner rigid wall of the mold and squeeze the finer particles of zeolite through the bottom effluent vent. Moreover the material was reused for each mass ratio mixtures. So the filter paper should be checked carefully to avoid losing the fine particles which the tested hydraulic conductivity value would be increased.

Typically the permeable reactive zone such as the permeable reactive barriers (PRBs) needed the uncompacted or slightly compacted materials with relatively high hydraulic conductivity which could remove the passing contaminant during seepage (Ören, 2013). The initial compactness of the uncompacted sample was another effect on the hydraulic conductivity tested value. But in these tests the degrees of the initial compactness for the uncompacted samples were not controlled precisely. The zeolite played the key role in the permeable reactive zone as a kind of ideal alternative material based on the relatively large permeability with high absorbability and cations exchange capacity (Mumpton, 1999; Park et al, 2002; Ören, 2013).

In contrast, the liner design, such as the landfill liner, needed as very low permeability as possible to effectively contain the liquids ( $1 \times 10^{-7}$  cm/s). Attributed to this test only the zeolite (clinoptilolite) and the ASTM 20-30 sand compacted mixtures were unable to be used as the impermeable layer. Some other finer particles materials with larger specific surface area and water holding capacity such as kaoline and bentonite were recommended to be added to amend the mixtures for reaching the standard.

### 3.3 Consolidation

The one-dimensional consolidation test was conducted to investigate the consolidation behaviors of the sand-zeolite mixtures samples. Three groups of uncompacted and compacted samples with different zeolite percentage (six samples) were prepared for the consolidation test. In order to compare the results, all the compacted samples were prepared with the maximum dry density (with optimum water content). Their compression index ( $C_c$ ), recompression index ( $C_r$ ), modulus of volume compressibility ( $m_v$ ), coefficient of consolidation ( $C_v$ ) were tested.

The influence of compaction effort and the effect of zeolite percentage on the mixtures consolidation behavior was discussed and analyzed below.

3.3.1 A representative results of the compression index and recompression index of Group 1 – 75% ASTM 20-30 sand and 25% zeolite mixtures

Table 3.4 The void ratio and strain information at 10.14% water content(OPT) of 75% ASTM 20-30 sand and 25% zeolite mixtures compacted sample (Representative)

<b>Vertical load(kPa)</b>	<b><math>\Delta H(\text{in})</math></b>	<b>Viod ratio e (<math>H-H_s</math>)/<math>H_s</math></b>	<b><math>\Sigma H(\text{in})</math></b>	<b><math>H(H_0-\Delta H)</math> (in)</b>	<b>Strain-<math>\epsilon</math> <math>\Sigma H/H_0(\%)</math></b>	
<b>0.00</b>	0.0000	$e_0$	<b>0.365</b>	0.0000	0.7500	<b>0.00</b>
<b>34.06</b>	0.0092	$e_1$	<b>0.349</b>	0.0092	0.7408	<b>1.23</b>
<b>68.11</b>	0.0036	$e_2$	<b>0.342</b>	0.0128	0.7464	<b>1.71</b>
<b>136.23</b>	0.0052	$e_3$	<b>0.333</b>	0.0180	0.7448	<b>2.40</b>
<b>272.45</b>	0.0055	$e_4$	<b>0.323</b>	0.0235	0.7445	<b>3.13</b>
<b>544.91</b>	0.0059	$e_5$	<b>0.312</b>	0.0294	0.7441	<b>3.92</b>
<b>1089.81</b>	0.0059	$e_6$	<b>0.301</b>	0.0353	0.7441	<b>4.71</b>
<b>Rebound</b>						
<b>544.91</b>	0.0011	$e_5'$	<b>0.303</b>	0.0342	0.7489	<b>4.56</b>
<b>272.45</b>	0.0013	$e_4'$	<b>0.305</b>	0.0329	0.7487	<b>4.39</b>
<b>136.23</b>	0.0014	$e_3'$	<b>0.308</b>	0.0315	0.7486	<b>4.20</b>
<b>68.11</b>	0.0014	$e_2'$	<b>0.311</b>	0.0301	0.7486	<b>4.01</b>
<b>34.06</b>	0.0015	$e_1'$	<b>0.313</b>	0.0286	0.7485	<b>3.81</b>
<b>0.00</b>	0.0045	$e_0'$	<b>0.322</b>	0.0241	0.7455	<b>3.21</b>

Table 3.4 showed some representative data of group 1 specimen. From the initial readings of the water content and the height of each specimen, initial void ratio volume of solid were calculated. The void ratio of each specimen at different level of loading was calculated based on the initial void ratio and deflection of the specimen. Table 3.4 showed the recorded void ratio and strain vs. the effective stress. It can be noticed that according to the data the vertical strain became larger as the effective stress increased but the growth was not proportional.

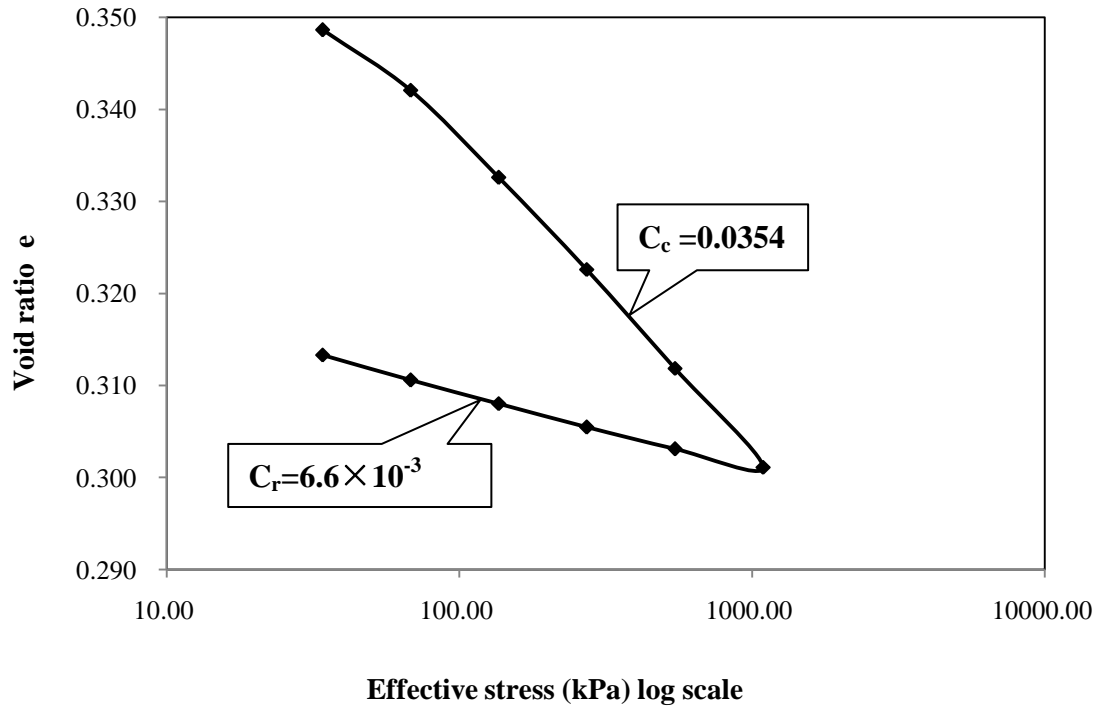


Figure 3.8 Effective stress (kPa) log scale vs. void ratio -  $e$  of 75% ASTM 20-30 sand and 25% zeolite mixtures at 10.14% water content of compacted sample

The relationship between void ratio and the effective stress (log scale) for the group1 compacted specimen was shown in Figure 3.8. The compression index  $C_c$  (the slope of the virgin compression curve) was determined as 0.0354, and the recompression index  $C_r$  was determined as  $6.6 \times 10^{-3}$  (the slope of recompression curve), using the following equations:

$$C_c = -\frac{e_2 - e_1}{\log \frac{\sigma_2}{\sigma_1}} \quad C_r = -\frac{e_2 - e_1}{\log \frac{\sigma_2}{\sigma_1}}$$

where:

$C_c$  = compression index,

$C_r$  = recompression index,

$e_{1,2}$  = void ratio, no units, and

$\sigma_{1,2}$  = effective stress, kPa.

As the figure 3.8 showed the  $C_c$  was larger than  $C_r$  which indicated that the sand and zeolite mixtures were nonconservative materials (Holtz, 1981; Ören, 2011) with the similar consolidation behavior of the soil.

After applying the load on the specimen the compressing force would squeeze the pore water out of the voids and this was the main reason for the settlement of the loaded specimen (Holtz and Kovacs, 1981). The testing specimen was installed in the odometer and fully saturated preparing for the consolidation test. And the specimen was assumed to be saturated even though it was difficult to reach 100% of saturation. So the compacted sample was soaked for a longer time to reach a higher degree of saturation.

The deflection of specimen was considered to be stable after applying the load for 24 hours. Since the specimen has relative low hydraulic conductivity, especially the compacted ones, it needed a long duration to fully finish the primary consolidation.

And due to the mixtures being modified samples there was not obvious pre-consolidation stress at the initial condition based on the Casagrande method.

### 3.3.2 Compression and recompression indices of all three groups tested samples

Table 3.5 Compression and recompression indices of all the testing samples

No.	$C_c$	$C_r$
<b>Group1 (25% Zeolite) compacted sample</b>	0.0354	0.0066
<b>Group2 (50% Zeolite) compacted sample</b>	0.0880	0.0133
<b>Group3 (75% Zeolite) compacted sample</b>	0.0831	0.0159
<b>Group1 (25% Zeolite) uncompact sample</b>	0.1063	0.0066
<b>Group2 (50% Zeolite) uncompact sample</b>	0.1986	0.0210
<b>Group3 (75% Zeolite) uncompact sample</b>	0.4664	0.0166

Table 3.5 summarized all the compression and recompression indices for all three groups of samples. In general, the compression index ( $C_c$ ) stood for the compressibility of the sand-zeolite mixtures. And the recompression index ( $C_r$ ) stood for the swelling potential of the deformation when the mixture samples were unloaded.

It was noticed that the  $C_c$  of the compacted sample was smaller than the uncompact sample of the same sand-zeolite mixture sample (e.g. see the slope of the virgin compression curve in *figure 3.9*). So a pre-compaction would significantly decrease the compressibility and volumetric deformation of the sand-zeolite mixtures.

However it was noted that the  $C_c$  of compacted sample in group3 was smaller than compacted sample in group2. As the zeolite content increased from 50% to 75% the compressibility of the sample decreased. It was not expected as the finer soil particles were more compressible than the medium sand. The observed less compressibility of high zeolite content specimen might due to the swelling ability of the zeolite. The swelling of the zeolite here by defined was the volumetric expansion of the mineral due to the contact with water, instead of the deformational rebound after unloading. And the swelling of zeolite mineral could be the reason for the less compressibility of group 3 samples. When the zeolite dominated the saturated consolidation sample (75% mass ratio) the swelling zeolite would partially undertake the consolidation force initially. But when the zeolite mass ratio was small (group 1) the swelling tendency was not significant enough to impact the settlement of the

specimen.

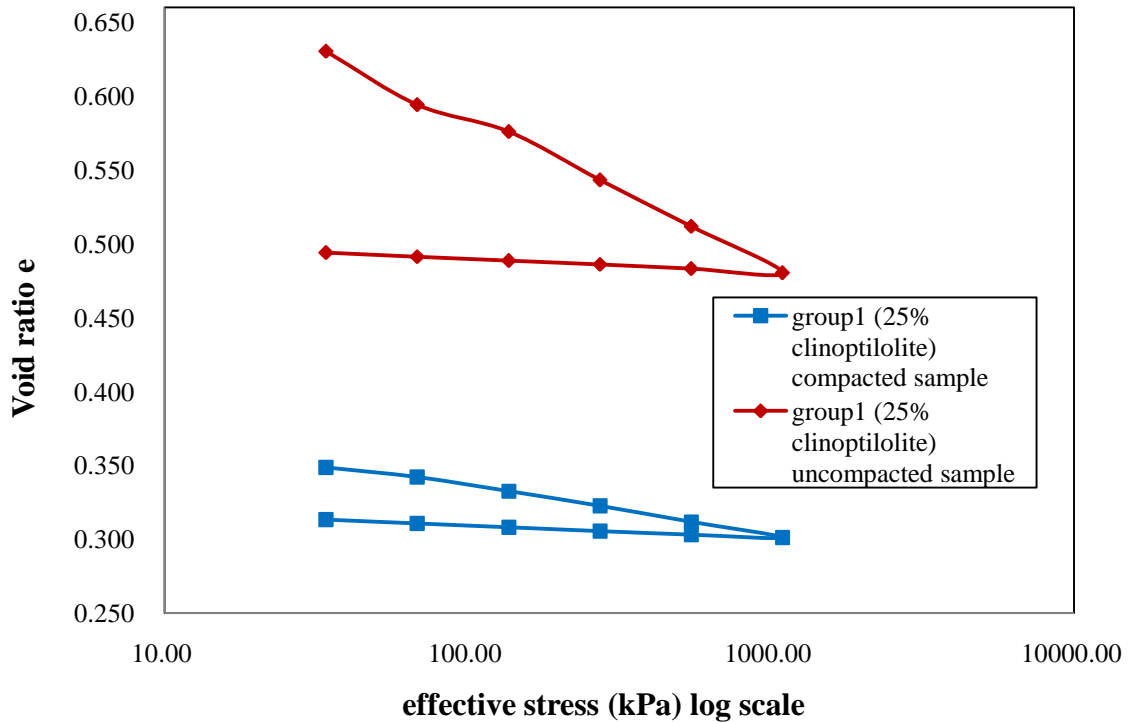


Figure 3.9 Comparison of the void ratio vs. effective stress between the compacted and uncompact samples in group1 (25% clinoptilolite)

Table 3.5 showed that the  $C_r$  values (also see the slopes of the recompression curves in figure 3.10 and figure 3.11) for the compacted and uncompact samples with same zeolite content were approximately same (same order of magnitude in group2). After high level of pressure (1089.81 kPa) were applied both the compacted and uncompact samples had insignificant amount of rebound, with higher amount of plastic deformation.

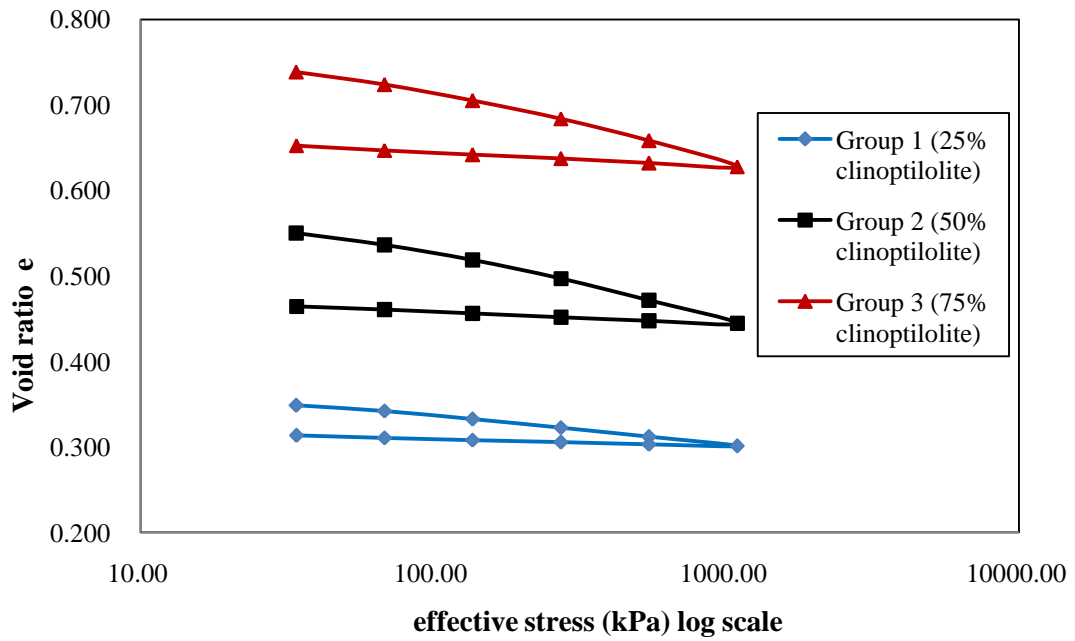


Figure 3.10 Three group consolidation of the compacted samples on OPT

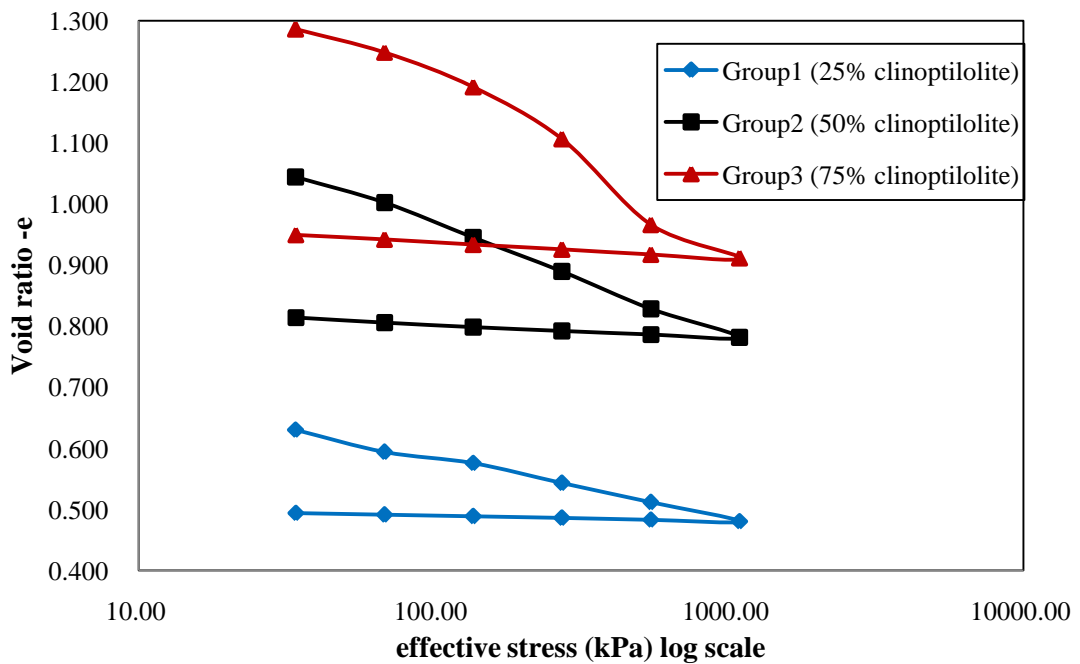


Figure 3.11 Three group consolidation of the uncompact samples with the same water content of each compacted OPT



### 3.3.3 The modulus of volume compressibility ( $m_v$ )

The modulus of volume compressibility ( $m_v$ ) was another index that indicated the compressibility of the sand-zeolite mixture sample using the following equations:

$$m_v = -\frac{\varepsilon_2 - \varepsilon_1}{\sigma_2 - \sigma_1}$$

where:

$m_v$  = modulus of volume compressibility,  $\frac{m^2}{kN}$ ,

$\varepsilon_{1,2}$  = vertical strain, no units, and

$\sigma_{1,2}$  = effective stress corresponding to the certain void ratio, kPa.

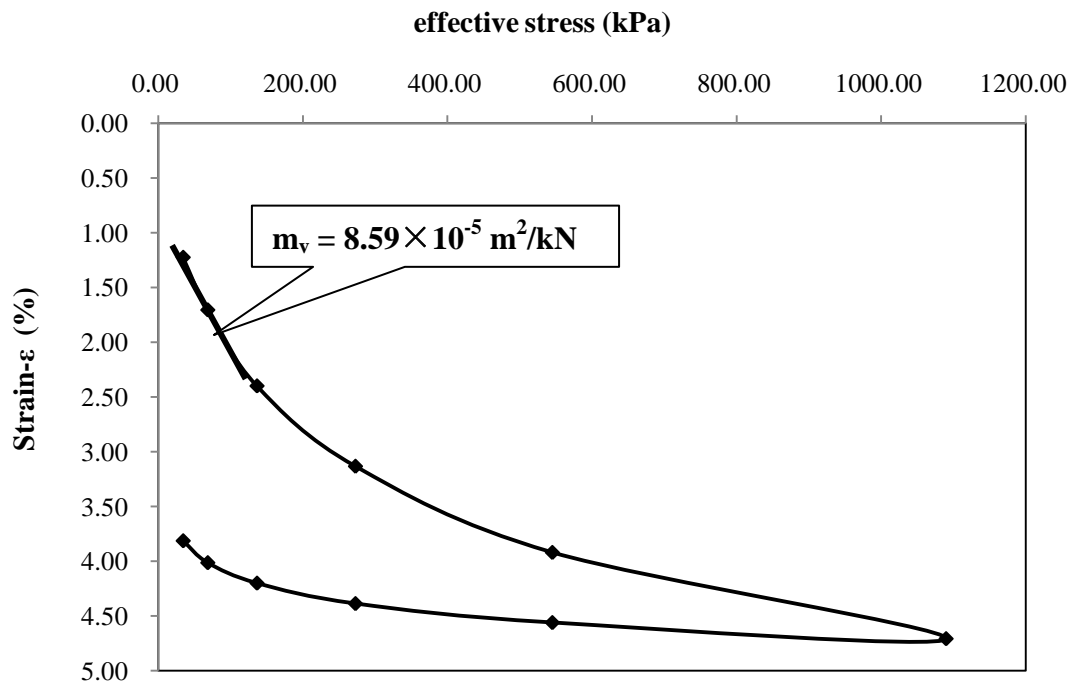


Figure 3.12 Effective stress (kPa) log scale vs. void ratio  $e$  of group 1(25% clinopilolite) with 10.14% water content (OPT) of compacted sample

Figure 3.12 indicated how  $m_v$  of group 1 (25% zeolite) with the OPT compacted sample was determined. In figure 3.12, the relationship between the stress and strain of the sand and zeolite mixture was obviously nonlinear. As the effective stress increased, the slope of stress-strain was decreased which showed the sand and zeolite mixtures were a strain hardening material (Holtz, 1981).

The initial slope of virgin compression was chosen to calculate the  $m_v$  for comparing the compressibility and stiffness of all the samples.

Table 3.6 The modulus of volume compressibility ( $m_v$ ) of all the three groups

<b>Name</b>	<b><math>m_v</math> (kN/m<sup>2</sup>)</b>
<b>group1 (25% Zeolite)compacted sample</b>	$1.15 \times 10^{-4}$
<b>group1 (25% Zeolite)uncompacted sample</b>	$3.61 \times 10^{-4}$
<b>group2 (50% Zeolite)compacted sample</b>	$1.92 \times 10^{-4}$
<b>group2 (50% Zeolite)uncompacted sample</b>	$3.99 \times 10^{-4}$
<b>group3 (75% Zeolite)compacted sample</b>	$1.84 \times 10^{-4}$
<b>group3(75% Zeolite)uncompacted sample</b>	$3.46 \times 10^{-4}$

Table 3.6 summarized the modulus of volume compressibility( $m_v$ )for all the samples. The larger the  $m_v$  value was, the higher the compressibility of the sample was. As shown in the data, the compaction effort decreased the compressibility of the sand-zeolite mixtures. The  $m_v$  of the uncompacted sample in group 1 was about 3 times than the compacted sample. And the  $m_v$  of uncompacted samples in group 2 & 3 was about twice the same compacted samples.

As the zeolite content increased from 25% to 50% the  $m_v$  increased significantly. But when the zeolite content increased from 50% to 75% the  $m_v$  decreased a little. Since the  $m_v$  here only indicated the initial compressibility, it was hard to make a conclusion for the compressibility over different stress levels. However, it was concluded that  $m_v$  of zeolite-sand mixture was less dependent on the percentage of zeolite.

### 3.3.4 The coefficient of consolidation ( $C_v$ )

The coefficient of consolidation ( $C_v$ ) indicated how fast the sand-zeolite mixtures consolidates under given effective stress.  $C_v$  was assumed a constant for each load increment. The  $C_v$  is an inherent property of the soil and it indicates the dissipation rate of excessive pore pressure.

There are two common methods to calculate the  $C_v$ : Casagrande method and Taylor method. Based on the data acquisitions it was hard to define the obviously secondary compression from the gage reading vs. log time curve (Casagrande method). So the Taylor method (Square root of time method) was used to determine the  $C_v$ .

Table 3.7 The Coefficient of Consolidation ( $C_v$ ) 10.14% water content(OPT) of 75% ASTM 20-30 sand and 25% zeolite mixtures compacted sample

Vertical load(kPa)	$\Delta H(\text{in})$	$\Sigma H(\text{in})$	$H(H_0-\Delta H)$ (in)	$H_{dr}$ (in)	$\sqrt{t_{90}}$ (min <sup>1/2</sup> )	$C_v(\text{mm}^2/\text{sec})$
<b>34.06</b>	0.0092	0.0092	0.7408	0.3727	1.7	<b>0.44</b>
<b>68.11</b>	0.0036	0.0128	0.7464	0.3718	2.1	<b>0.29</b>
<b>136.23</b>	0.0052	0.0180	0.7448	0.3728	1.3	<b>0.75</b>
<b>272.45</b>	0.0055	0.0235	0.7445	0.3723	1.4	<b>0.64</b>
<b>544.91</b>	0.0059	0.0294	0.7441	0.3722	1.2	<b>0.88</b>
<b>1089.81</b>	0.0059	0.0353	0.7441	0.3721	1.5	<b>0.56</b>

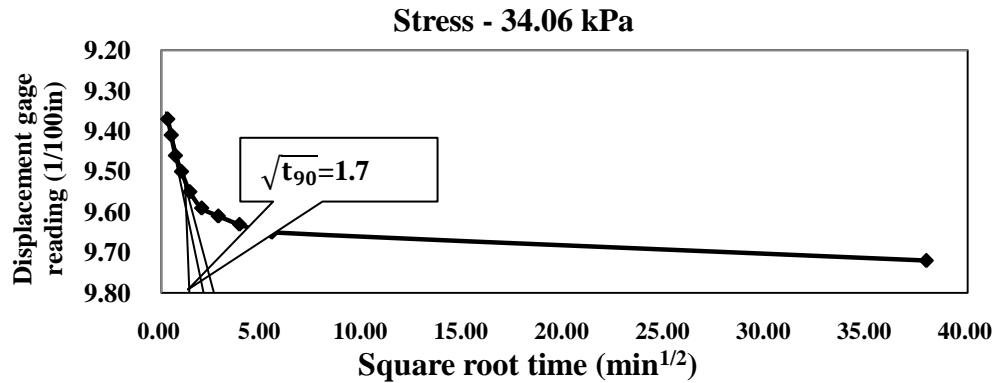


Figure 3.13 The representative of square root time curve method of group 1 (75% ASTM 20-30 sand and 25% zeolite mixtures) at 10.14% water content of compacted sample

Table 3.7 and figure 3.13 showed examples of calculated coefficients of consolidation ( $C_v$ ). The  $C_v$  value was a constant at each effective stress level. The larger the values of  $C_v$  increased, the higher the speed rate of consolidations were. Figure 3.13 showed how to use the Taylor method to calculate the  $C_v$  for one increment of the effective stress. The procedure was to extrapolate the linear portion of the displacement gage reading curve to intercept the coordinate axis. The value of the intercepting point on the square root time axis was enlarged by 15%. And then a new straight line was plotted from the new value enlarged point to the origin point of the displacement curve. The new line intercepted with the displacement curve and a vertical line was plotted from the intercepting point to the coordinate axis. So the  $\sqrt{t_{90}}$  value could be acquired from the chart. And the  $C_v$  could be calculated by the equation mentioned in the method chapter.

Table 3.8 The Coefficient of Consolidation ( $C_v$ ) of all the consolidation samples

$C_v(\text{mm}^2/\text{sec})$		
<b>Vertical load(kPa)</b>	<b>Group1(25% Zeolite) compacted samples</b>	<b>Group1(25% Zeolite) uncompact samples</b>
<b>34.06</b>	0.44	2.51
<b>68.11</b>	0.29	1.80
<b>136.23</b>	0.75	1.37
<b>272.45</b>	0.64	2.99
<b>544.91</b>	0.88	1.61
<b>1089.81</b>	0.56	2.02
<b>Vertical load(kPa)</b>	<b>Group2(50% Zeolite) compacted samples</b>	<b>Group2(50% Zeolite) uncompact samples</b>
<b>34.06</b>	0.55	1.98
<b>68.11</b>	0.73	3.50
<b>136.23</b>	0.87	1.98
<b>272.45</b>	1.03	0.75
<b>544.91</b>	1.24	1.26
<b>1089.81</b>	0.86	1.97
<b>Vertical load(kPa)</b>	<b>Group3(75% Zeolite) compacted samples</b>	<b>Group3(75% Zeolite) uncompact samples</b>
<b>34.06</b>	0.64	0.65
<b>68.11</b>	0.48	0.47
<b>136.23</b>	0.87	0.89
<b>272.45</b>	1.04	0.69
<b>544.91</b>	1.54	0.75
<b>1089.81</b>	3.45	1.06

Table 3.8 summarized all the  $C_v$  values of all the consolidation testing samples. Take the group 1 (25% Zeolite) for instance, for the same mixtures the uncompact sample had obviously larger  $C_v$  than the compacted sample at each effective stress. The uncompact samples had the faster rate of the consolidation. As the discussion above the uncompact mixture sample of group 1 had larger hydraulic conductivity than the compacted one. In the consolidation test the applying load forced the pore water out and rearrange the soil matrix into a stronger one. And the hydraulic conductivity controlled the rate of the drainage, the rate of pressure dissipation and consequently, the rate of consolidation.

The  $C_v$  values of group 2 (50% zeolite) were also determined and they also showed similar trend that the uncompact sample had the faster rate of the

consolidation than the compacted sample of the same mixture (except the point of 272.45 kPa effective stress).

However for group 3 samples, the uncompacted sample had the same rate of the consolidation with the compacted sample under the lower effective stress level. And under the higher effective stress the uncompacted sample even had a slower rate of the consolidation. A phenomenon was observed that the sample with higher zeolite content (75% zeolite) would swell in the rigid mold after the hydraulic conductivity test. The height of the sample would increase in the mold after contact with enough water after a while. When the zeolite swelled, the consolidation force would overcome both the swelling force and the excess pore water pressure simultaneously. It was expected that the swelling of mixture samples would prevail as zeolite content increased. The similar coefficients of consolidation for group 3 samples suggested that the compaction effort, which typically would reduce the swelling tendency of zeolite particles, might not exert such significant influence on sand/zeolite mixtures with very high zeolite content.

### 3.3.5 The relationships between the effective stress and strain of all three groups tested samples

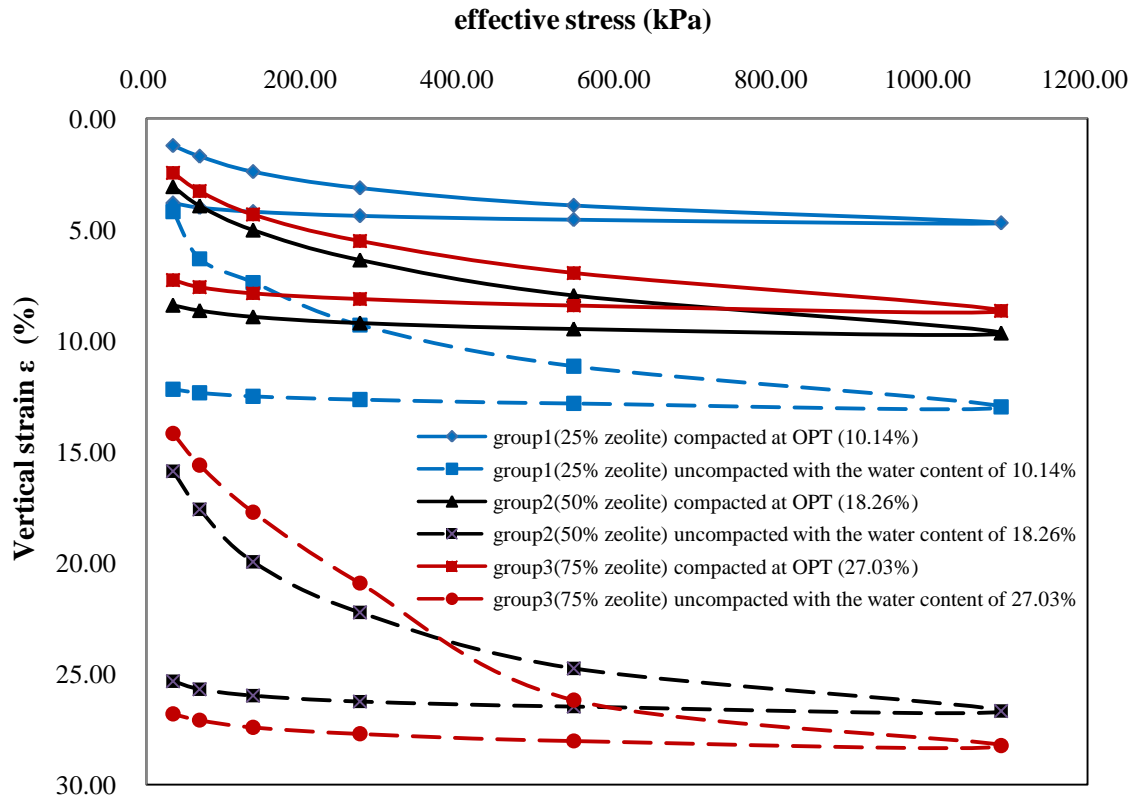


Figure 3.14 Comparison of the strain and effective stress of three groups OPT compacted samples and the same water content uncompacted samples

The figure 3.14 summarized the relationships of vertical strain vs. effective stress for all the consolidation testing samples. From the figure it was noticed that each uncompacted sample apparently had the larger strain under the same effective stress as the compacted sample of the same sand-zeolite mixture. But the compacted sample of group 2 (50% zeolite) had larger strain than the compacted sample of group 3 (75% zeolite) under the same effective stress. Similarly the uncompacted sample of group 2 (50% zeolite) also had larger strain than the compacted sample of group 3 (75% zeolite) under a larger effective stress level. In general the zeolite as a finer particle soil should have higher compressibility than the medium sand. Here the water might result in the swelling of the zeolite since the swelling of the sand was negligible. As the

specific surface area of the clinoptilolite was just relatively large ( $40\text{m}^2/\text{g}$ , Hong, 2012) its swelling ability was not significantly strong. There was not considerable swelling phenomenon between the 25% mass ratio of the zeolite in the mixtures and 50%. But when the zeolite dominated the mixtures (75%) the swelling became significant, which affected the compression index  $C_c$  and the coefficient of consolidation  $C_v$ . Additional tests of the swelling ability of the zeolite minerals were recommended for the future study.



## 4. SUMMARY AND CONCLUSION

The scope of this thesis was to investigate the compactive behavior; conduction and compressibility of sand and zeolite mixtures. It was motivated by their applications as reactive materials in permeable reactive barriers, liners and vertical cutoff walls. The impact of different percentage of zeolite on the engineering behaviors on zeolite/ASTM20-30 sand was investigated. Based on obtained laboratory results this study provided following conclusions:

For compaction behavior:

1. Zeolite had relatively larger specific surface area and smaller specific gravity than the ASTM 20-30 sand, so based on the same compaction method (Proctor compaction) as the zeolite mass ratio increasing in the mixtures the optimum water content would increase and the maximum dry unit weight would decrease.

2. For zeolite/sand mixtures with their water content equal to or greater than OPT, the degrees of saturation tended to be larger as the zeolite percentage of the mixtures increased from 25% to 75%.

For hydraulic conductivity behavior:

3. The compacted sand/zeolite specimen had lowest hydraulic conductivity near the OPT. All tested specimen with water content higher than OPT had relatively lower hydraulic conductivities.

4. The compacted sand /zeolite mixtures had relatively larger hydraulic conductivities on dry side of the OPT. The initial water content and degree of saturation were essential for the measured hydraulic conductivities of compacted sand/zeolite mixtures.

5. Compaction effort significantly decreased the hydraulic conductivity of sand/zeolite mixtures at all levels of zeolite percentage.

6. For the uncompacted samples the tested hydraulic conductivity values tended to be reduced by approximately one order of magnitude while the zeolite (clinoptilolite) percentage increased every 25% in the mixtures (From 0% to 75%). But for the compacted samples at the optimum water content, the impact of zeolite percentage on the hydraulic conductivity was not significant and the measured hydraulic conductivities were typically in the same order of magnitude.

For consolidation behavior:

7. Compaction effort significantly decreased the compressibility of sand-zeolite mixtures at all levels of zeolite percentage.

8. As the zeolite percentage of mixtures increased from 25% to 50% the compressibility of the tested samples were increased. As the zeolite percentage of mixtures increased from 50% to 75% the compressibility of the tested samples decreased.

9. With low zeolite content, the uncompacted sand/zeolite samples had obviously faster rate of consolidation than the compacted samples. With high zeolite content, the uncompacted sand/zeolite samples had approximately the same rate of consolidation as the compacted samples.

## 5. SUGGESTION FOR FUTURE STUDY

The following are suggested to further enhance the understanding of the geotechnical properties of the sand/zeolite mixtures as an engineered reactive filter/sorptive material.

1. Different types of natural zeolite need to be tested and compared to evaluate the similarities and differences on the geotechnical/geochemical properties.

2. Impact of different permeant fluid with varying density and viscosity on the fluid conduction should be evaluated. Especially when zeolite have stronger tendency of swelling in such liquids.

3. For the application of permeable reactive barriers, the interaction between specific zeolite and environmental contaminants should be studied. The removal mechanism of a variety of contaminants by zeolite, including sorption and filtration merit examination.

4. On the basis of 3, interaction kinetics of zeolite vs. contaminants should be examined. For contaminant flow progresses rapidly in sand-zeolite mixture, the removal percentage of contaminants will be a function of flow time in the medium if interaction equilibrium is not reached (due to high conduction rate or low detention time).

## REFERENCES

ASTM standard methods:

ASTM D422-07 Standard test method for particle-size analysis of soils.

ASTM D854-10 Standard test methods for specific gravity of soil solids by water pycnometer.

ASTM D698-07 Standard methods for laboratory compaction characteristics of soil using standard effort (12,400 ft-lbf/ft<sup>3</sup> (600kN-m/m<sup>3</sup>))

ASTM D5856-95 (Reapproved 2007) Standard test method for measurement of hydraulic conductivity of porous material using a rigid-wall, compaction-mold permeameter.

ASTM D2435-04 Standard test methods for one-dimensional consolidation properties of soils using incremental loading.

Textbooks:

Bekku, H. v. (2001). Introduction to zeolite science and practice (2nd completely rev. and expanded Ed.). Amsterdam; New York: Elsevier.

Budhu, M. (2011). Soil mechanics and foundations (3rd Ed.). New York: Wiley.

Dyer, A. (1988). An introduction to zeolite molecular sieves. Chichester; New York: J. Wiley.

Gillham, R.; Vogan, J.; Gui, L.; Duchene M.; Son J. (2010). Iron barrier walls for chlorinated solvent remediation. In: Stroo, H. F.; Ward, C. H. (eds.), In Situ Remediation of Chlorinated Solvent Plumes. Springer Science + Business Media, New York, NY

Holtz, R. D., & Kovacs, W. D. (1981). An introduction to geotechnical engineering. Englewood Cliffs, N.J.: Prentice-Hall.

National Research Council (1997). Innovations in ground water and soil cleanup-- From concept to commercialization: Washington, D.C., National Academies Press

Todd, D. K., & Mays, L. W. (2005). Groundwater hydrology (3rd Ed.). Hoboken, NJ: Wiley.

Journal articles or thesis:

Aksoy, Y. Y. (2010). Characterization of two natural zeolites for geotechnical and geoenvironmental applications. Applied Clay Science.

Altare, C. R., Bowman, R. S., Katz, L. E., Kinney, K. A., & Sullivan, E. J. (2007). Regeneration and long-term stability of surfactant-modified zeolite for removal of volatile organic compounds from produced water. Microporous and Mesoporous Materials.

Belbase, S., Urynowicz, M. A., Vance, G. F., & Dangi, M. B. (2013). Passive remediation of coalbed natural gas co-produced water using zeolite. J Environ Manage.

Bruch, I., Fritsche, J., Banninger, D., Alewell, U., Sendelov, M., Hurlimann, H. Alewell, C. (2011). Improving the treatment efficiency of constructed wetlands with zeolite-containing filter sands. *Bioresour Technol.*

Czurda, KA; Haus, R.(2002). Reactive barriers with fly ash zeolites for in situ groundwater remediation, *Applied Clay Science*

Dangi, M. B., Urynowicz, M. A., & Belbase, S. (2013). Characterization, generation, and management of household solid waste in Tulsipur, Nepal. *Habitat International.*

Fronczyk J. (2008). Zeolite-sand mixtures in permeable reactive barriers in landfill's surrounding. Doctoral thesis, Department of Geotechnical Engineering, WULS, Warsaw (in Polish).

Hedström. A. (2006). Reactive filter materials for ammonium and phosphorus sorption in small scale wastewater treatment, Doctoral thesis, Department of Civil and Environmental Engineering, Division of Architecture and Infrastructure.

Hong, C. S., Shackelford, C. D., & Malusis, M. A. (2012). Consolidation and Hydraulic Conductivity of Zeolite-Amended Soil-Bentonite Backfills. *Journal of Geotechnical and Geoenvironmental Engineering.*

Joanna, F., & Kazimierz, G. (2013). Evaluation of zeolite-sand mixtures as reactive materials protecting groundwater at waste disposal sites. *Journal of Environmental Sciences.*

Jorgensen, T. C., & Weatherley, L. R. (2003). Ammonia removal from wastewater by ion exchange in the presence of organic contaminants. *Water Research.*

Kovalick, W.J.(1999). *Field Applications of In Situ Remediation Technologies:*

Permeable Reactive Barriers. U.S. Environmental Protection Agency

Lee S. H., Jo H. Y., Yun S. T. and Lee Y. J. (2010). Evaluation of factors affecting performance of zeolitic rock barrier to remove zinc from water. *Journal of Hazardous Materials*.

Li, S., et al. (2014). Ammonium removal from groundwater using a zeolite permeable reactive barrier: a pilot-scale demonstration. *Water Sci Technol*.

Ly, G., Li, Z., Jiang, W.-T., Ackley, C., Fenske, N., & Demarco, N. (2014). Removal of Cr(VI) from water using Fe(II)-modified natural zeolite. *Chemical Engineering Research and Design*.

Maretto, M., Bianchi, F., Vignola, R., Canepari, S., Baric, M., Iazzoni, R., Papini, M. P. (2014). Microporous and mesoporous materials for the treatment of wastewater produced by petrochemical activities. *Journal of Cleaner Production*.

Ören, A. H., Durukan, S., & Kayalar, A. Ş. (2014). Influence of compaction water content on the hydraulic conductivity of sand-bentonite and zeolite-bentonite mixtures. *Clay Minerals*.

Ören, A. H., Kaya, A., & Kayalar, A. S. (2011). Hydraulic conductivity of zeolite-bentonite mixtures in comparison with sand-bentonite mixtures. *Canadian Geotechnical Journal*.

Ören, A. H., & Ozdamar, T. (2013). Hydraulic conductivity of compacted zeolites. *Waste Manag. Res*.

Park J. B, Lee S. H., Lee J. W. and Lee C. Y. (2002) Lab scale experiments for permeable reactive barriers against contaminated groundwater with ammonium and

heavy metals using clinoptilolite. *Journal of Hazardous Materials*.

Piñón-Villarreal, A. R., Bawazir, A. S., Shukla, M. K., & Hanson, A. T. (2013). Retention and Transport of Nitrate and Ammonium in Loamy Sand Amended with Clinoptilolite Zeolite. *Journal of Irrigation and Drainage Engineering*.

Scherer, M. M.; Richter, S.; Valentine, R. L.; Alvarez P. J. J. (2000). Chemistry and microbiology of permeable reactive barriers for in situ groundwater clean-up. *Critical Reviews in Environmental Science and Technology*.

Sivasankar, V., & Ramachandramoorthy, T. (2011). Water softening behaviour of sand materials—mimicking natural zeolites in some locations of Rameswaram Island, India. *Chemical Engineering Journal*.

Tounsi, H., Mseddi, S., & Djemel, S. (2009). Preparation and characterization of Na-LTA zeolite from Tunisian sand and aluminum scrap. *Physics Procedia*.

Tratnyek, P. G.; M. M. Scherer; T. J. Johnson; Matheson, L.J. (2003). Permeable reactive barriers of iron and other zero-valent metals. In: Tarr M. A. (ed.), *Chemical Degradation Methods for Wastes and Pollutants; Environmental and Industrial Applications*. *Environmental Science and Pollution Control*.

United States Environmental Protection Agency (1998). *Permeable Reactive Barrier Technologies for Contaminant Remediation*. Office of Research and Development Washington DC.

Valdes, H., Farfan, V. J., Manoli, J. A., & Zaror, C. A. (2009). Catalytic ozone aqueous decomposition promoted by natural zeolite and volcanic sand. *J Hazard Mater*.



## APPENDIX

### Abbreviations:

$A$  = cross-sectional area of specimen

$a$  = cross-sectional area of the reservoir containing the influent liquid

$C_c$  = compression index

$C_r$  = recompression index

$D$  = diameter of the specimen

$e$  = void ratio

$e_0$  = initial void ratio

$e_{1,2}$  = void ratio

$G_s$  = specific gravity

$H_0$  = initial specimen height

$H_{dr}$  = length of the drainage path

$H_f$  = final specimen height

$H_s$  = height of the solid

$h$  = difference in hydraulic head across the specimen

$h_1$  = head loss across the specimen, at time  $t_1$

$h_2$  = head loss across the specimen at time  $t_2$

$k$  = hydraulic conductivity

$t$  = interval of time

$t$  = elapsed time between determination of  $h_1$  and  $h_2$

$L$  = length of specimen along path of flow

$m_v$  = modulus of volume compressibility

$M_d$  = mass of dry soil

$S$  = saturation degree

$T$  = a dimensionless time factor

$t_{90}$  = time corresponding to the particular degree of consolidation

$V$  = volume of the test specimen or quantity of flow

$V_v$  = volume of voids in soil

$V_s$  = volume of solids in soil

$V_T$  = total volume of soil

$w$  = water content

ZAV = zero air void

$\sigma_{1,2}$  = effective stress

$\epsilon_{1,2}$  = vertical strain

$\gamma_w$  = unit weight of water

$\gamma_d$  = dry unit weight

$\rho_w$  = wet density of the soil mixture sample

$\rho_d$  = dry density of the soil mixture sample

$\rho_m$  = moist density of the soil mixture sample

$\rho_s$  = density of the solid

*Some representative tables for different tests:*

Table I Data analysis for the particle distribution of ASTM 20-30 sand

<b>Sieve No.</b>	<b>Sieve size(mm)</b>	<b>Mass of soil retained (g)</b>	<b>Mass retained on Sieve(%)</b>	<b>Cumulative retained (%)</b>	<b>Percent Finer Than Each Sieve(%)</b>
<b>20</b>	0.850	92	18.39	18.39	81.61
<b>30</b>	0.600	403	80.54	98.92	1.08
<b>40</b>	0.420	3	0.68	99.61	0.39
<b>60</b>	0.250	1	0.29	99.90	0.10
<b>80</b>	0.175	0	0.07	99.97	0.03
<b>100</b>	0.150	0	0.01	99.98	0.02
<b>140</b>	0.106	0	0.01	100.00	0.00
<b>200</b>	0.075	0	0.00	100.00	0.00
<b>pan</b>	0.000	0	0.00	100.00	0.00

Table II Data analysis for the particle distribution of zeolite (clinoptilolite)

<b>Sieve No.</b>	<b>Sieve size(mm)</b>	<b>Mass of soil retained (g)</b>	<b>Mass retained on Sieve(%)</b>	<b>Cumulative retained(%)</b>	<b>Percent Finer Than Each Sieve(%)</b>
<b>40</b>	0.420	0	0.00	0.00	100.00
<b>60</b>	0.250	2	0.52	0.52	99.48
<b>80</b>	0.175	2	0.69	1.21	98.79
<b>100</b>	0.150	9	3.04	4.26	95.74
<b>140</b>	0.106	87	29.01	33.27	66.73
<b>200</b>	0.075	144	47.85	81.12	18.88
<b>pan</b>	0.000	57	18.88	100.00	0.00

Table III Specific Gravity of ASTM20-30

<b>Test No.</b>	<b>1</b>	<b>2</b>	<b>3</b>	<b>4</b>	
<b>Pycnometer No.</b>	1	2	3	4	
<b>Norminal Volume (ml)</b>	100	100	100	100	
<b>Temperature degree(°C)</b>	20	20	20	20	
<b>W<sub>1</sub> (grams)</b>	155.67	156.45	156.21	160.64	
<b>W<sub>d</sub> (grams)</b>	9.25	8.66	6.73	7.98	
<b>W<sub>1</sub> + W<sub>d</sub>(grams)</b>	164.92	165.11	162.94	168.62	
<b>W<sub>2</sub> (grams)</b>	161.45	161.86	160.39	165.64	
<b>W<sub>1</sub> + W<sub>d</sub>- W<sub>2</sub>(grams)</b>	3.47	3.25	2.55	2.98	<b>Average</b>
<b>γ<sub>s</sub> (grams/cm3)</b>	2.670	2.669	2.644	2.683	<b>2.67</b>
<b>G<sub>s</sub></b>	2.675	2.674	2.649	2.687	<b>2.67</b>

Table IV Specific Gravity of zeolite

<b>Test No.</b>	<b>1</b>	<b>2</b>	<b>3</b>	<b>4</b>	
<b>Pycnometer No.</b>	1	2	3	5	
<b>Norminal Volume (ml)</b>	100	100	100	100	
<b>Temperature degree (°C)</b>	20	20	20	20	
<b>W<sub>1</sub> (grams)</b>	155.7	156.42	156.2	139.83	
<b>W<sub>d</sub> (grams)</b>	2.79	3.68	4.2	4.55	
<b>W<sub>1</sub> + W<sub>d</sub>(grams)</b>	158.49	160.1	160.4	144.38	
<b>W<sub>2</sub> (grams)</b>	157.28	158.52	158.62	142.39	
<b>W<sub>1</sub> + W<sub>d</sub>- W<sub>2</sub>(grams)</b>	1.21	1.58	1.78	1.99	<b>Average</b>
<b>γ<sub>s</sub> (grams/cm3)</b>	2.310	2.333	2.364	2.291	<b>2.32</b>
<b>G<sub>s</sub></b>	2.314	2.337	2.368	2.295	<b>2.33</b>

Table V The data acquisition of the first group compaction test

Test	1	2	3	4	5	6	7
Mass of mold and base(g)	3717	3717	3717	3717	3717	3717	3717
Mass of mold and base+ compacted soil(g)	5434	5539	5588	5658	5820	5795	5730
Mass of compacted soil in the mold(g)	1717	1822	1871	1941	2103	2078	2013
$\rho$ of the moisture soil(g/cm <sup>3</sup> )	1.77	1.88	1.93	2.00	2.17	2.14	2.08
Moisture can No.	G1-11	G1-9	G1-9	G1-9	G1-6	G1-2	G1-10
Mass of moisture container(g)	14.81	14.90	14.75	14.9	14.76	14.61	14.74
Mass of container+wet soil(g)	52.16	28.39	36.6	38.55	24.54	32.37	35.07
Mass of container+dry soil(g)	50.45	27.61	35.19	36.87	23.64	30.53	32.62
Mass of soil(g)	35.64	12.71	20.44	21.97	8.88	15.92	17.88
Mass of water(g)	1.71	0.78	1.41	1.68	0.9	1.84	2.45
Water content w(%)	<b>4.80</b>	<b>6.14</b>	<b>6.90</b>	<b>7.65</b>	<b>10.14</b>	<b>11.56</b>	<b>13.70</b>
Mass of dry soil in the mold(g)	1638.4	1716.7	1750.3	1803.1	1909.5	1862.7	1770.4
$\rho_d$ (g/cm <sup>3</sup> )	1.69	1.77	1.81	1.86	1.97	1.92	1.83
$\gamma_d$ (kN/m <sup>3</sup> )	<b>16.58</b>	<b>17.37</b>	<b>17.71</b>	<b>18.25</b>	<b>19.33</b>	<b>18.85</b>	<b>17.92</b>
$\gamma_d$ of ZAV(kN/m <sup>3</sup> )	22.55	21.88	21.51	21.17	20.09	19.52	18.72

Table VI The basic data of hydraulic conductivity test at 4.80% water content of 75% ASTM 20-30 sand and 25% zeolite mixtures compacted sample

<b>Water content - w (%)</b>	<b>4.80</b>
Dry density $\rho_d$ (g/cm <sup>3</sup> )	1.69
Mass of mold(g)	3717
Mass of mold and soil(g)	5434
Mass of soil in the mold(g)	1717
Diameter of the sample (in)	4
Diameter of the sample (in)	4
Area of the cross-section(m <sup>2</sup> )	0.00810732
Constant head	114 cm 1.14 m
Vertical distance of the sample	4.714 in 0.1197356 m

Table VII The data acquisition of hydraulic conductivity test at 4.80% water content of 75% ASTM 20-30 sand and 25% zeolite mixtures compacted sample

<b>Test Number</b>	<b>1</b>	<b>2</b>	<b>3</b>	<b>4</b>	<b>5</b>	<b>6</b>
Time to accumulate water(s)	125.08	131.3	166.13	118.63	121.28	121.31
Mass of beaker (g)	153.83	277.5	261.76	401.63	408.63	108.23
Mass of beaker + water(g)	181.63	305.62	295.94	427.16	433.85	133.31
Mass of water(g)	27.8	28.12	34.18	25.53	25.22	25.08

Table VIII The test result of hydraulic conductivity at 4.80% water content of 75% ASTM 20-30 sand and 25% zeolite mixtures compacted sample

<b>K<sub>1</sub>(m/s)</b>	<b>K<sub>2</sub>(m/s)</b>	<b>K<sub>3</sub>(m/s)</b>	<b>K<sub>4</sub>(m/s)</b>	<b>K<sub>5</sub>(m/s)</b>	<b>K<sub>6</sub>(m/s)</b>	<b>Average of K(m/s)</b>	<b>Average of K(cm/s)</b>
$2.88 \times 10^{-6}$	$2.77 \times 10^{-6}$	$2.67 \times 10^{-6}$	$2.79 \times 10^{-6}$	$2.69 \times 10^{-6}$	$2.68 \times 10^{-6}$	$2.75 \times 10^{-6}$	$2.75 \times 10^{-4}$

Table IX The basic data of hydraulic conductivity test at 10.14 % water content(OPT) of 75% ASTM 20-30 sand and 25% zeolite mixtures compacted sample

<b>Water content - w (%)</b>	<b>11.56</b>	
Dry density $\rho_d(g/cm^3)$	1.92	
Mass of the compaction mold(g)	3717	
Mass of the compaction mold and remaining soil(g)	5795	
Mass of soil in the compaction mold(g)	2071	
Height of the soil sample in the compaction mold(sample height)	4.714 in	11.97356 cm
Diameter of the compaction mold	4 in	10.16 cm
Diameter of the monometer (cm)	0.466	
A-area of the sample (cm <sup>2</sup> )	81.0732	
a-area of the monometer (cm <sup>2</sup> )	0.1706	
Head difference between 0 scale and effluent (cm)	22.8	

Table X The data acquisition and result of hydraulic conductivity test at 10.14% water content of 75% ASTM 20-30 sand and 25% zeolite mixtures compacted sample

Test No.	h of read at the begin(cm)	h <sub>1</sub> (cm)	h of read at the end(cm)	h <sub>2</sub> (cm)	Time(s)	K(cm/s)	K(m/s)
1	69.15	91.95	68.70	91.50	583.10	2.12×10 <sup>-7</sup>	2.12×10 <sup>-9</sup>
2	68.70	91.50	67.00	89.80	2249.17	2.10×10 <sup>-7</sup>	2.10×10 <sup>-9</sup>
3	67.00	89.80	66.45	89.25	756.80	2.04×10 <sup>-7</sup>	2.04×10 <sup>-9</sup>
4	66.45	89.25	66.00	88.80	635.77	2.00×10 <sup>-7</sup>	2.00×10 <sup>-9</sup>
5	66.00	88.80	65.35	88.15	918.33	2.02×10 <sup>-7</sup>	2.02×10 <sup>-9</sup>
6	65.35	88.15	65.05	87.85	414.03	2.07×10 <sup>-7</sup>	2.07×10 <sup>-9</sup>
7	65.05	87.85	28.00	50.80	68605.40	2.01×10 <sup>-7</sup>	2.01×10 <sup>-9</sup>
<b>Average</b>						<b>2.05×10<sup>-7</sup></b>	<b>2.05×10<sup>-9</sup></b>

Where h<sub>1</sub>= h of read at the begin + h<sub>0</sub>

h<sub>2</sub>= h of read at the begin + h<sub>0</sub>

h<sub>0</sub>= head difference between 0 scale and effluent

Table XI The data acquisition and result of hydraulic conductivity test at 18.26% (OPT)water content of 75% ASTM 20-30 sand and 25% zeolite mixtures compacted sample

Test No.	h of read at the begin(cm)	h <sub>1</sub> (cm)	h of read at the end(cm)	h <sub>2</sub> (cm)	Time(s)	k(cm/s)	k(m/s)
1	97.20	120.00	96.70	119.50	604.41	1.74×10 <sup>-7</sup>	1.74×10 <sup>-9</sup>
2	96.70	119.50	96.15	118.95	645.20	1.80×10 <sup>-7</sup>	1.80×10 <sup>-9</sup>
3	96.15	118.95	95.50	118.30	618.78	2.23×10 <sup>-7</sup>	2.23×10 <sup>-9</sup>
4	95.50	118.30	94.95	117.75	625.72	1.88×10 <sup>-7</sup>	1.88×10 <sup>-9</sup>
5	94.95	117.75	94.40	117.20	618.01	1.91×10 <sup>-7</sup>	1.91×10 <sup>-9</sup>
6	94.40	117.20	93.85	116.65	610.39	1.94×10 <sup>-7</sup>	1.94×10 <sup>-9</sup>
7	93.85	116.65	93.30	116.10	619.21	1.92×10 <sup>-7</sup>	1.92×10 <sup>-9</sup>
<b>Average</b>						<b>1.92×10<sup>-7</sup></b>	<b>1.92×10<sup>-9</sup></b>

## CURRICULUM VITA

NAME: Hong Shang

ADDRESS: Department of Civil and Environmental Engineering  
132 Eastern Parkway  
University of Louisville  
Louisville, KY 40292

DOB: Tianjin city, China- March 31, 1984

### EDUCATION

& TRAINING: B.S., Civil Engineering  
Tongji University  
2002-2006

M.S., Civil Engineering  
University of Louisville  
2014-2015

AWARDS: The first prize of survey and design in  
CIGIS (Limited) China, 2008